Supporting Information

Supramolecular Self-assembled Polymeric Nanospheres Based on Hydrazino Naphthalimide Functionalised Pillar[5]arene for Long Chain Aldehyde Detection

Yanisa Sanguansap,[a] Vithaya Ruangpornvisuti,[a] Thassanant Atithep,[b] Thanthapatra Bunchuay,[c*] Boosayarat Tomapatanaget[a*]

[a]Department of Chemistry, Faculty of Science, Chulalongkorn University, Bangkok, 10330, Thailand
[b]Vidyasirimedhi Institute of Science and Technology (VISTEC) Wangchan Valley 555 Moo 1 Payupnai, Wangchan, Rayong 21210 Thailand
[c]Department of Chemistry and Center of Excellence for Innovation in Chemistry (PERCH-CIC), Faculty of Science, Mahidol University, Bangkok, 10400, Thailand

[a*]E-mail: boosayarat.t@chula.ac.th and tboosayarat@gmail.com
[c*]E-mail: thanthapatra.bun@mahidol.edu and thanthapatra.bunchuay@gmail.com

Table of Contents

1.	Materials and analytical instruments	Page 2
2.	Synthesis and characterization of fluorescence probe HNP5A	Page 3
3.	Synthesis and characterization of fluorescence probe HNOB	Page 19
4.	Host-guest complexation studies of HNP5A⊂C9 in DMSO-d_6 by ^{1}H NMR titration, 2D NOESY NMR and HRMS (ESI) techniques	Page 29
5.	pH and time variation for guests detection procedure by fluorescence spectrophotometry	Page 31
6.	Selectivity study of HNP5A towards various aldehyde compounds by fluorescence spectrophotometry	Page 32
7.	Sensitivity study of HNP5A towards C9 and C8 by fluorescence spectrophotometry	Page 33
8.	Interference study in the process of C9 detection	Page 34
9.	Sensitivity study of HNP5A⊂C9 towards Ag ions (Ag^+) by fluorescence spectrophotometry	Page 35
10.	Particle size verification of HNP5A, HNP5A⊂C9, and AgNPs-HNP5A⊂C9 by DLS measurement	Page 37
11.	Morphology characterization and size distribution of HNP5A, HNP5A⊂C9, HNP5A + Ag^+, and AgNPs-HNP5A⊂C9 by FESEM and HRTEM techniques	Page 38
12.	DFT Optimized structures and reaction energies	Page 40
13.	References	Page 44

1. Materials and analytical instruments

1.1 Materials

All reagents and solvents for synthesis were purchased from Tokyo Chemical Industry (TCI), Sigma-Aldrich, RCI Labscan, and Merck and used without further purification. Deuterated solvents for NMR analysis were bought from Cambridge Isotope Laboratories. For the analytical process, all substances for preparing buffer solution and aldehyde compounds were obtained from TCI, Sigma-Aldrich, and Carlo Erba. All metal ions used as analytes were obtained from Sigma-Aldrich. Dimethyl sulfoxide as a spectroscopic grade for fluorescence measurement was received from Merck and used without drying.

1.2 Analytical instruments

The ^{1}H NMR spectra were recorded by JEOL (500 MHz), Bruker AVANCE 400 spectrometer (400 MHz), Bruker AVANCE 500 spectrometer (500 MHz), while ^{13}C NMR spectra were recorded on the same machine (100 MHz) at 298K. The peak assignments were acquired by NMR experiments including DEPT-135, ^{1}H-^{13}C heteronuclear single-quantum coherence (HSQC), 2D Nuclear Over Hauser Enhancement Spectroscopy (NOESY). MALDI-TOF mass spectra were carried out on Bruker Daltonics MALDI-TOF by using α-hydroxy cyanocinnamic acid (CCA) as a matrix. High-Resolution Mass Spectra (HRMS) were collected data with a Bruker MicrOTOF Q-II MS instrument with ESI, positive mode and Bruker maXis UHR-TOF (Ultra High Resolution-TOF), ESI. Fourier transform infrared (FT-IR) spectrophotometric measurements were obtained by using a Thermo Scientific, Nicolet 6700 FT-IR spectrometer. All fluorescence spectra were measured by a Varian Cary Eclipse Probe fluorescence spectrophotometer by personal computer data processing unit. The light source is Cary Eclipse a pulsed xenon lamp and a detector is a photomultiplier tube. The morphology and size of nanoparticles were determined by scanning electron microscope (SEM) of a Hitachi SU8010 at an operational voltage of 10 kV. High-resolution transmission electron microscopy (HRTEM) images and scanning transmission electron microscope-energy-dispersive X-ray (STEM-EDX) spectroscopy were performed by a JEOL JEM-ARM 200F with a Gantan detector and a field emission gun operated at 200 kV accelerating voltage. Dynamic light scattering (DLS) was collected by using Mastersizer S and Zetasizer nanoseries instruments (Mulvern Instrument).

2. Synthesis and characterization of fluorescence probe HNP5A

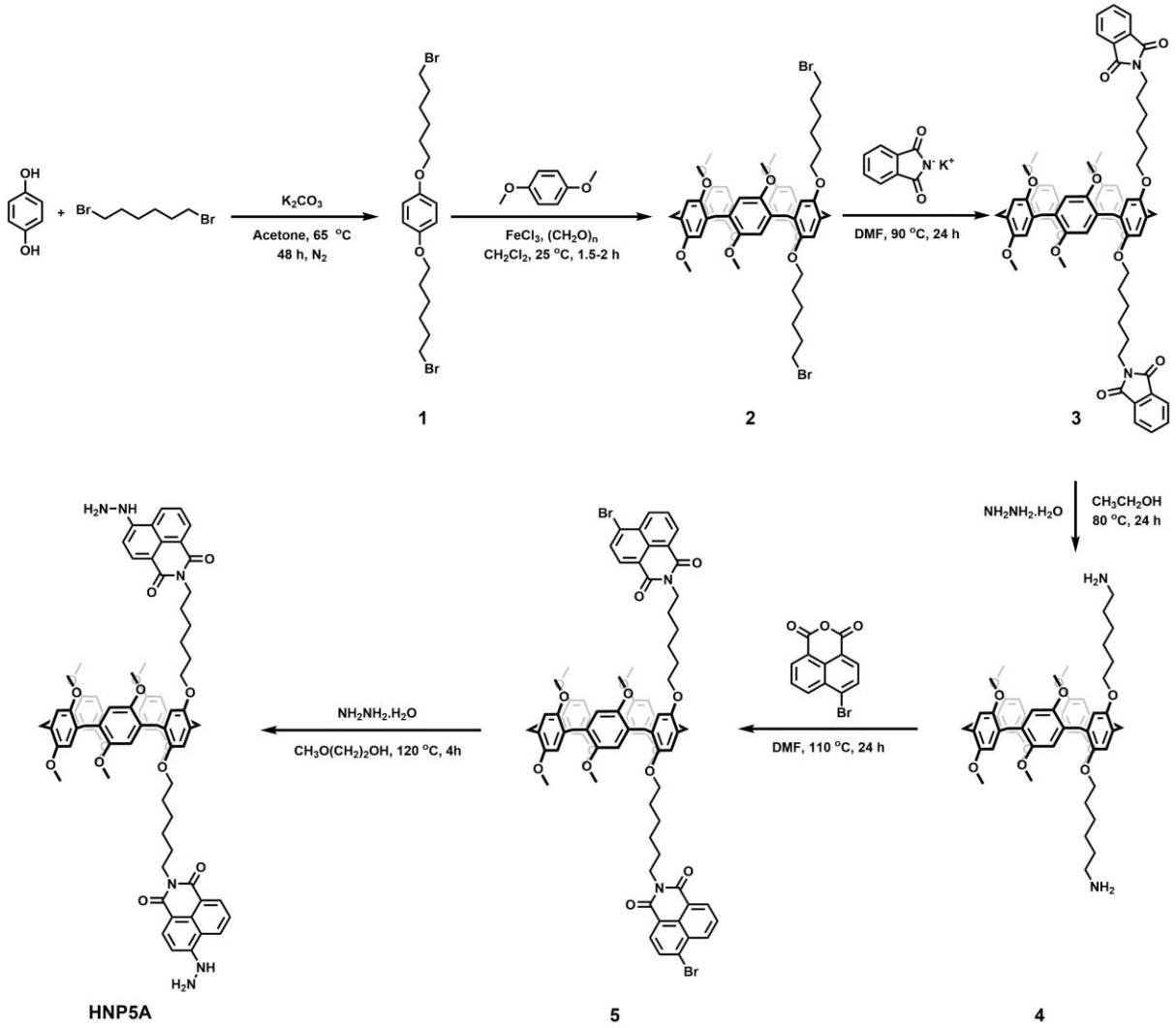

Figure S1 Synthesis pathway of **HNP5A**.

2.1 Synthesis of 1,4-bis((6-bromohexyl)oxy)benzene (1)

1

According to the literature procedure[1] to synthesize monomer **1**, hydroquinone (1.376 g, 12.5 mmol) and potassium carbonate (10.365 g, 75.0 mmol) were dissolved in dried acetone (50 mL) under a nitrogen atmosphere. The mixture solution was degassed by nitrogen gas for one hour. 1,6-dibromohexane was added to the reaction and refluxed for 48 hours under the nitrogen system. Potassium carbonate (15.38 mL, 100.0 mmol) was filtrated. The precipitate was washed with dichloromethane. The solution was evaporated under reduced pressure. After the solvent was removed, the crude product was purified by column chromatography with 30-50% dichloromethane/hexane to obtain product **1** as a white solid (4.54 g, 83.3% yield).

^{1}H NMR [500 MHz, $CDCl_3$] δ 6.81 (s, 4H), 3.91 (t, *J* = 6.4 Hz, 4H), 3.42 (t, *J* = 6.9 Hz, 4H), 1.92 – 1.86 (m, 4H), 1.80 – 1.74 (m, 4H), 1.51 – 1.48 (m, 8H).

^{13}C NMR [126 MHz, $CDCl_3$] δ 153.22, 115.46, 68.43, 53.57, 34.00, 32.79, 32.60, 29.30, 28.04, 27.39, 25.41.

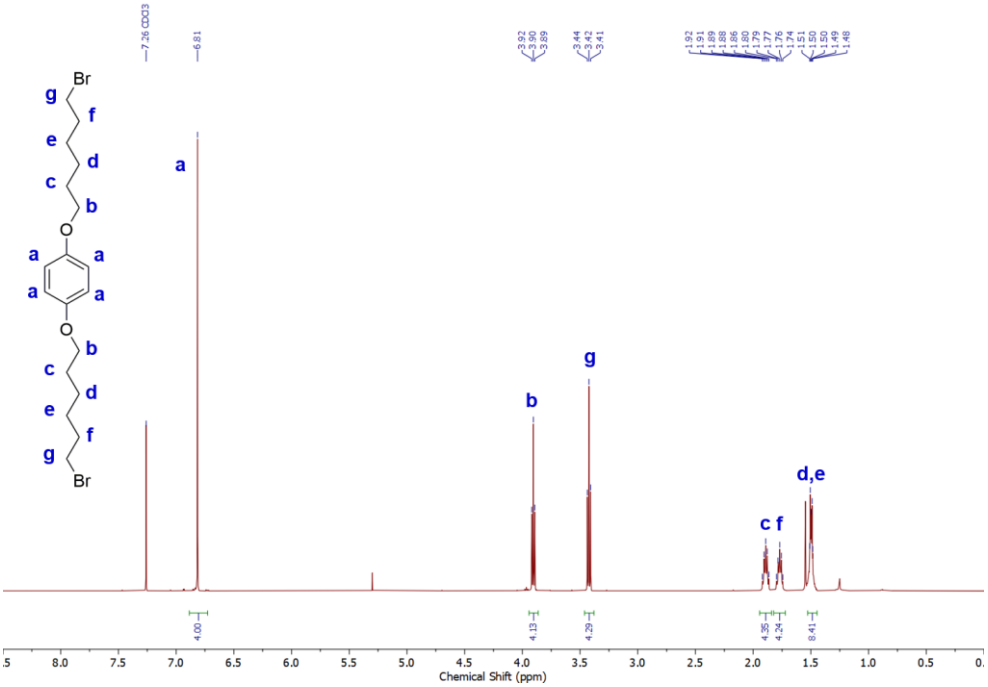

Figure S2 ^{1}H NMR spectrum (500 MHz, $CDCl_3$, 298 K) of **1**.

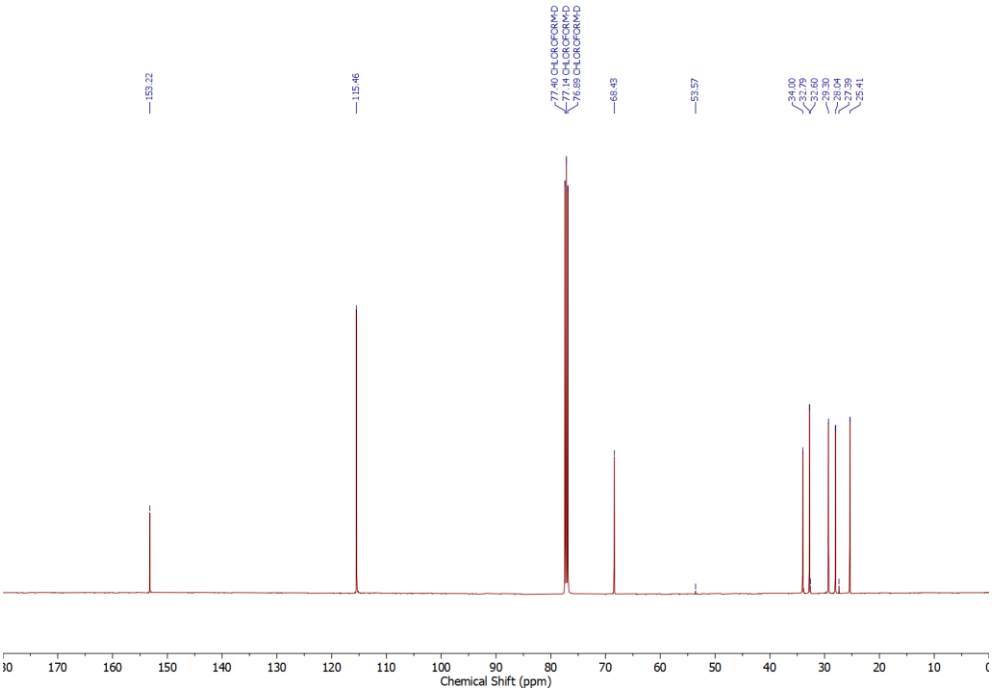

Figure S3 ^{13}C NMR spectrum (126 MHz, $CDCl_3$, 298 K) of **1**.

2.2 Synthesis of copillar[5]arene (2)

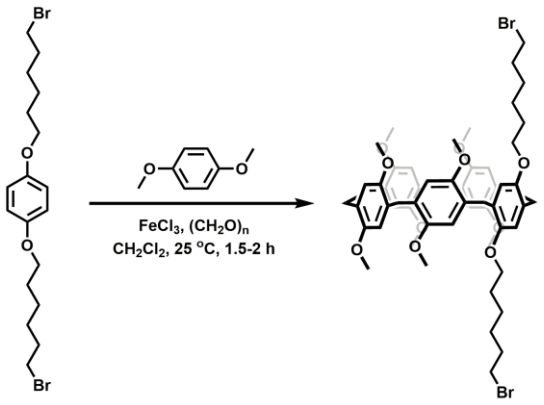

1 **2**

The synthetic method of molecule **2** was modified from prior research.[2] Monomer **1** (0.545 g, 1.25 mmol) and 1,4-dimethoxybenzene (2.764 g, 20 mmol) were dissolved in dried dichloromethane (400 mL). Paraformaldehyde (1.801 g, 60 mmol) was added to the mixture solution under nitrogen gas. Anhydrous ferric chloride was added to the reaction and the mixture solution was stirred at 25-30 °C. After the complete reaction, deionized water was added to quench the reaction. The crude product was extracted with dichloromethane (3 × 20 mL). The combined organic phase was dried over anhydrous sodium sulfate. The crude product was purified by column chromatography with 50% dichloromethane/hexane to acquire **2** as a white solid (0.4247 g, 32.4% yield)

^{1}H NMR [500 MHz, $CDCl_3$] δ 6.95 – 6.87 (m, 10H), 3.91 – 3.75 (m, 42H), 2.24 – 1.66 (m, 4H), 1.37 – 1.24 (m, 8H), 0.88 – 0.82 (m, 4H).

^{13}C NMR [126 MHz, $CDCl_3$] δ 150.50, 150.28, 150.24, 149.64, 128.14, 128.08, 127.88, 114.14, 113.14, 112.94, 68.28, 55.36, 55.30, 33.59, 32.03, 30.09, 29.81, 29.37, 29.20, 29.15, 27.90, 23.55, 22.81, 14.25.

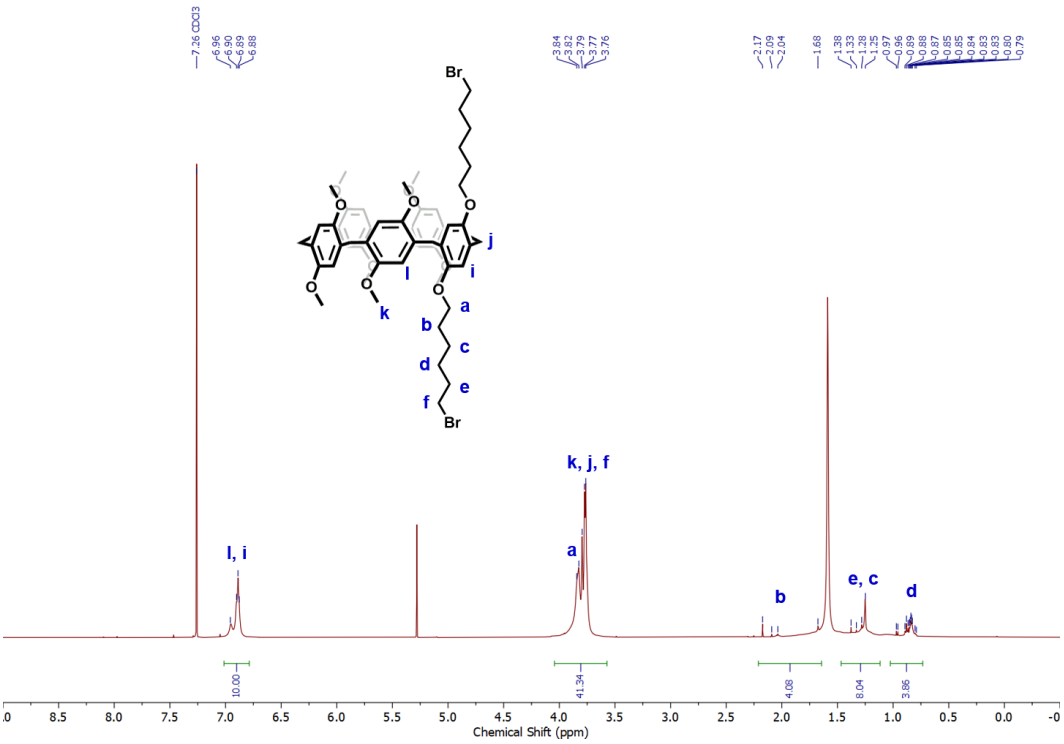

Figure S4 ^{1}H NMR spectrum (500 MHz, $CDCl_3$, 298 K) of **2**.

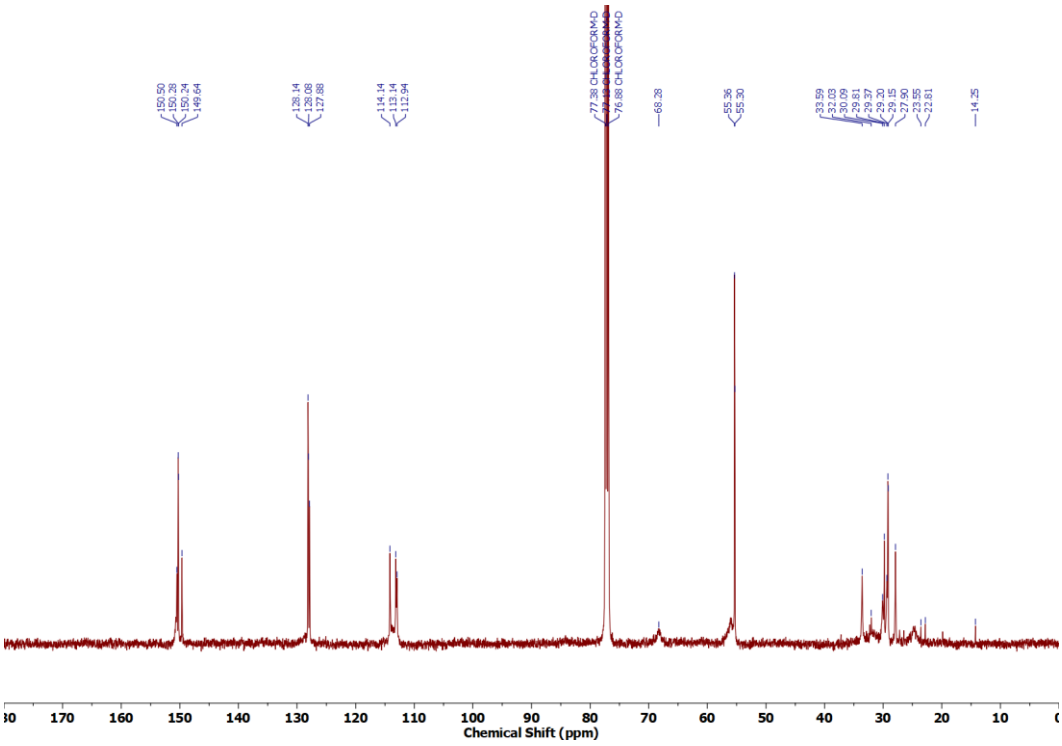

Figure S5 ^{13}C NMR spectrum (126 MHz, $CDCl_3$, 298 K) of **2**.

2.3 Synthesis of bis-phthalimide copillar[5]arene (3)

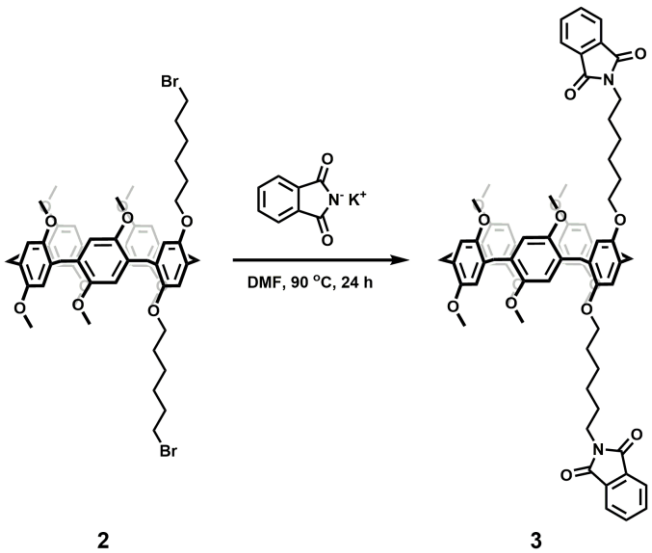

2 **3**

A mixture of **2** (0.40 g, 0.38 mmol) and potassium phthalimide (0.21 g, 1.13 mmol) was dissolved in dimethylformamide (3.00 mL). The suspension was refluxed at 90 °C for 24 hours. After cooling to room temperature, the dichloromethane and residue dimethylformamide was evaporated following adding of toluene and chloroform, respectively. The crude product was extracted with dichloromethane and deionized water several times and brine last time, then dried over anhydrous

sodium sulfate. The solvent was removed under reduced pressure to receive product **3** as a yellow solid (quantitative yield).

^{1}H NMR [500 MHz, $CDCl_3$] δ 7.88 – 7.83 (m, 4H), 7.74 – 7.70 (m, 4H), 6.76 – 6.73 (m, 10H), 3.82 – 3.60 (m, 4H), 1.83 – 1.69 (m, 4H), 1.57 – 1.53 (m, 4H), 1.46 – 1.40 (m, 4H), 1.28 – 1.21 (m, 4H).

^{13}C NMR [126 MHz, $CDCl_3$] δ 168.60, 167.96, 166.96, 162.66, 150.87, 150.78, 150.74, 150.04, 134.51, 134.43, 134.03, 132.71, 132.20, 131.75, 128.43, 128.31, 128.28, 128.11, 128.06, 125.12, 123.88, 123.71, 123.30, 114.95, 114.25, 114.04, 113.98, 68.38, 55.92, 55.88, 55.82, 53.18, 40.49, 38.05, 37.21, 36.30, 32.29, 31.99, 31.38, 30.17, 29.86, 29.79, 29.62, 29.58, 29.49, 28.72, 27.22, 26.92, 26.49, 26.10, 23.55, 22.77, 14.25.

HRMS (ESI) m/z: [$C_{71}H_{76}N_2O_{14}$ + H^+]$^+$ calcd for 1181.5369; Found 1181.5361.

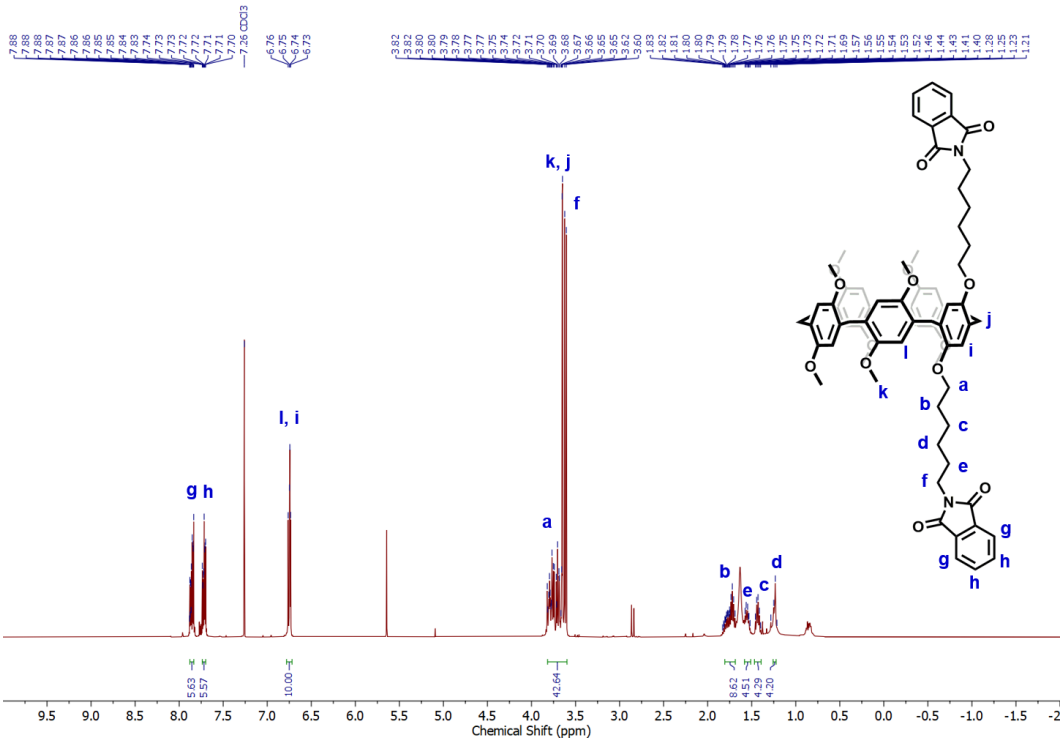

Figure S6 ^{1}H NMR spectrum (500 MHz, $CDCl_3$, 298 K) of **3**.

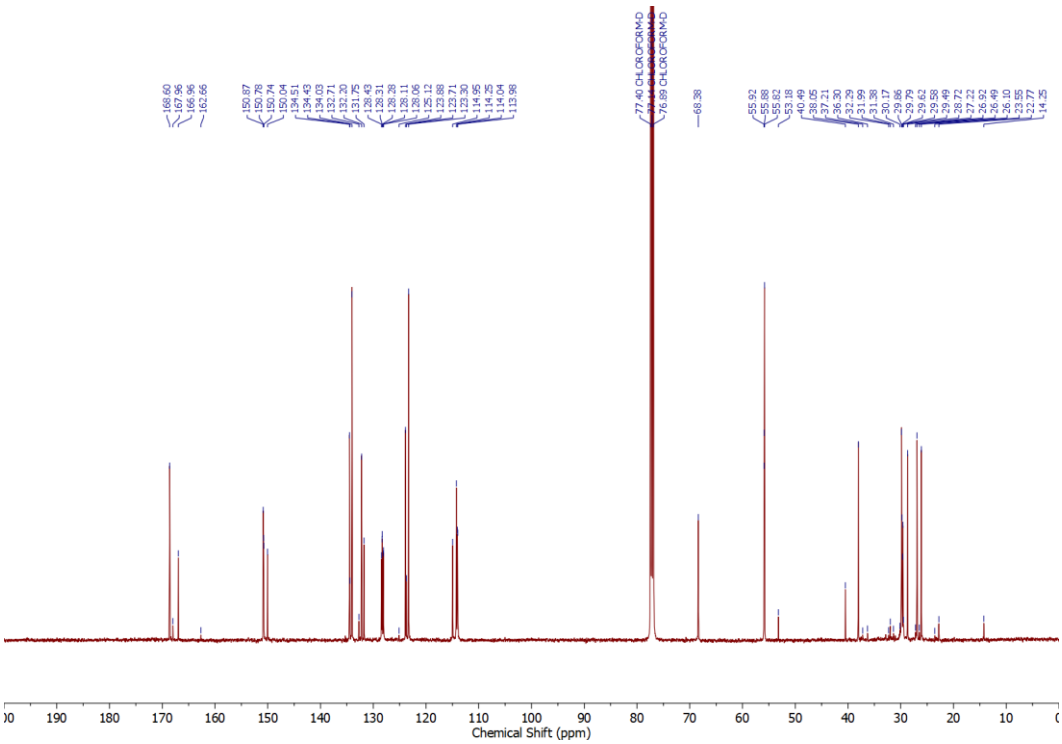

Figure S7 ^{13}C NMR spectrum (126 MHz, $CDCl_3$, 298 K) of **3**.

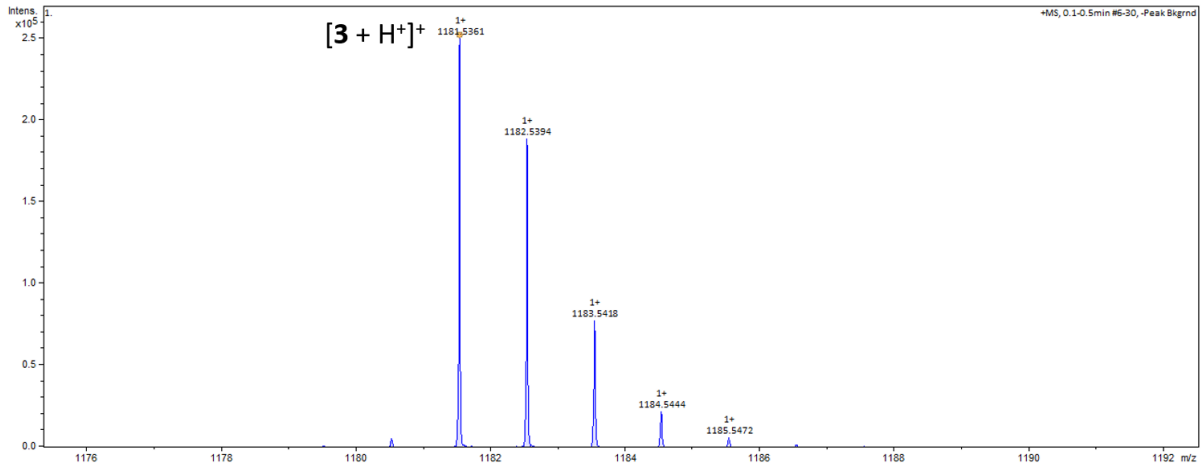

Figure S8 HRMS-ESI mass spectrum of **3**.

2.4 Synthesis of bis-amino copillar[5]arene (4)

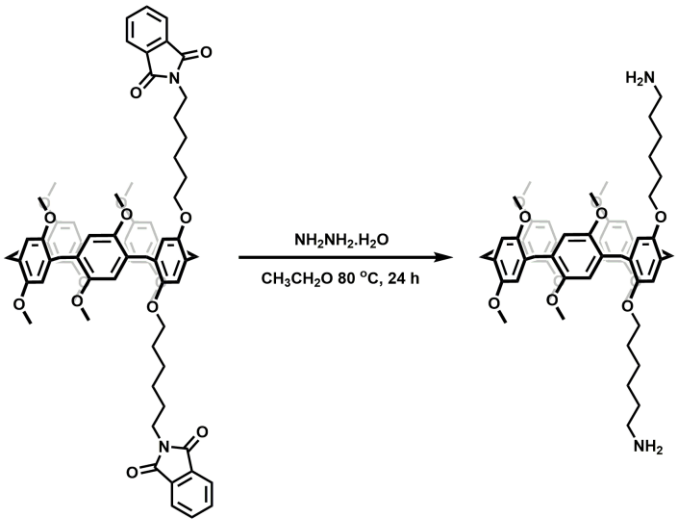

3 4

Product **3** (0.76 g, 0.64 mmol) was dissolved in ethanol (20 mL) under nitrogen gas. Hydrazine monohydrate (0.62 mL, 12.83 mmol) was subsequently added to produce a white solid and the suspension was stirred at 80 °C overnight. The mixture solution was evaporated to remove hydrazine and ethanol. The crude product was dissolved in dichloromethane and washed with deionized water (3 × 50.00 mL) and brine (50.00 mL), then dried over anhydrous sodium sulfate and the solvent was removed under reduced pressure to obtain product **4** as a white solid (0.45 g, 75.73% yield)

^{1}H NMR [500 MHz, $CDCl_3$] δ 6.90 – 6.86 (m, 10H), 3.95 (t, *J* = 6.6 Hz, 4H), 3.84 – 3.70 (m, 38H), 1.68 – 1.66 (m, 4H), 1.38 – 1.25 (m, 8H), 0.89 – 0.83 (m, 4H).

^{13}C NMR [126 MHz, $CDCl_3$] δ 150.68, 150.55, 150.47, 150.44, 149.68, 128.86, 128.43, 128.35, 128.23, 114.87, 114.32, 113.61, 113.52, 113.48, 68.95, 56.27, 55.91, 55.82, 55.73, 41.04, 37.19, 32.29, 32.03, 31.91, 29.81, 29.58, 29.26, 29.01, 26.08, 25.41, 22.80, 14.25.

HRMS (ESI) m/z: $[C_{55}H_{72}N_2O_{10} + H^+]^+$ calcd for 921.5260; Found 921.5233.

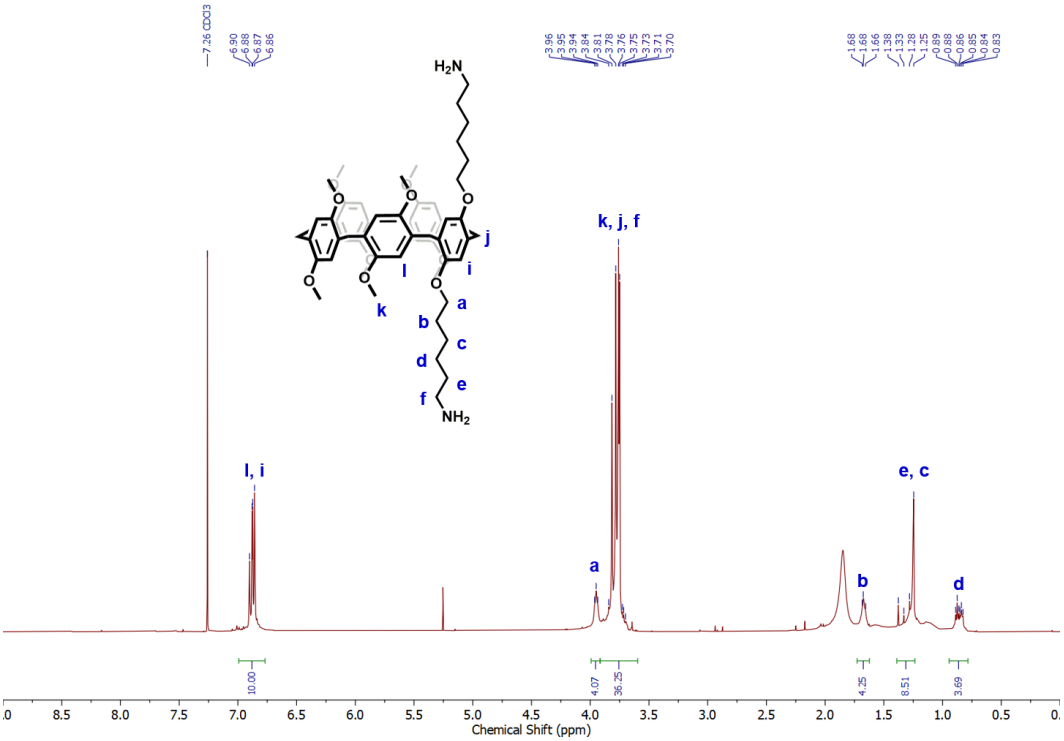

Figure S9 ^{1}H NMR spectrum (500 MHz, $CDCl_3$, 298 K) of **4**.

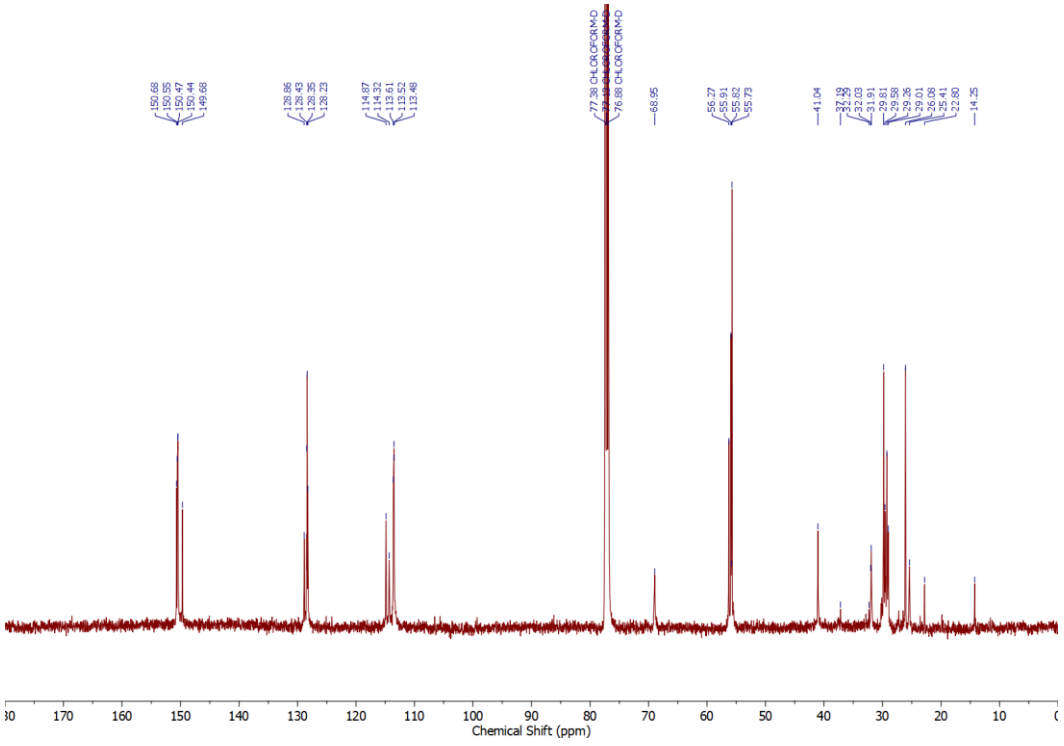

Figure S10 ^{13}C NMR spectrum (126 MHz, $CDCl_3$, 298 K) of **4**.

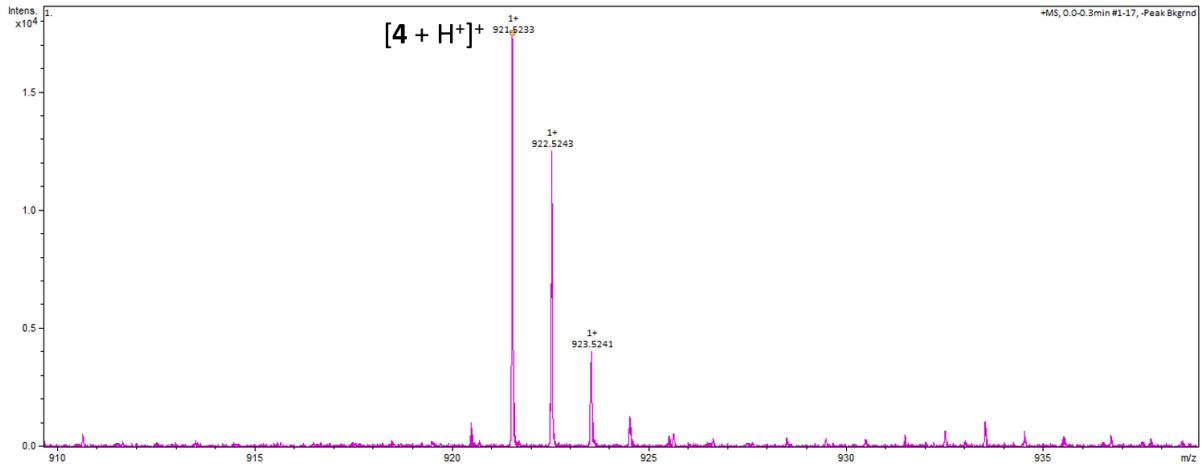

Figure S11 HRMS-ESI mass spectrum of **4**.

2.5 Synthesis of bis-bromo napthlimide copillar[5]arene (5)

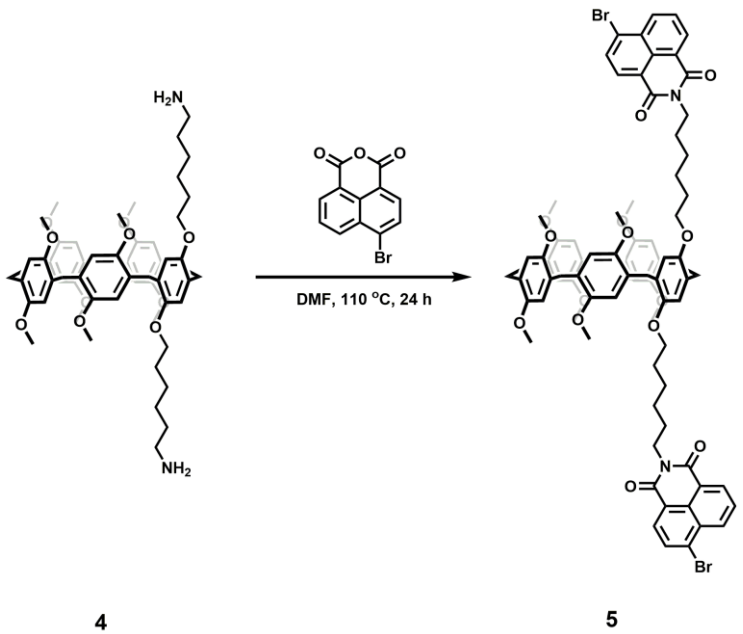

4 **5**

A mixture of product **4** (0.45 g, 0.49 mmol) and 4-bromo-1,8-naphthalic anhydride (0.40 g, 1.46 mmol) was dissolved in DMF (2.00 mL). The reaction solution was refluxed under nitrogen for 24 hours, the dimethylformamide was removed to a minimum amount under reduced pressure. The mixture was dissolved in dichloromethane and extracted with deionized water several times, brine, and dried over anhydrous sodium sulfate. The solvent was removed in vacuo. The crude product was purified by column chromatography using dichloromethane/hexane (70-100% v/v) to acquire product **5** as a yellow solid (0.55 g, 77.86% yield).

^{1}H NMR [500 MHz, $CDCl_3$] δ 8.66 (d, *J* = 7.2 Hz, 2H), 8.57 (d, *J* = 8.6 Hz, 2H), 8.41 (d, *J* = 7.7 Hz, 2H), 8.04 (d, *J* = 8.0 Hz, 2H), 7.85 (t, *J* = 7.9 Hz, 2H), 6.75 – 6.72 (m, 10H), 4.20 (t, *J* = 7.6 Hz, 4H), 3.82 – 3.70 (m, 14H), 3.67 – 3.60 (m, 24H), 1.84 – 1.75 (m, 8H), 1.53 – 1.50 (m, 4H), 1.29 – 1.24 (m, 4H).

^{13}C NMR [126 MHz, $CDCl_3$] 163.77, 163.74, 150.84, 150.73, 150.01, 135.33, 133.39, 132.15, 131.34, 131.20, 130.72, 130.39, 129.09, 128.42, 128.25, 128.19, 128.11, 127.98, 123.16, 122.30, 114.85, 114.19, 113.98, 68.42, 60.54, 55.88, 55.82, 55.79, 53.24, 40.58, 32.29.

HRMS (ESI) m/z: $[C_{79}H_{78}Br_2N_2O_{14} + H^+]^+$ calcd for 1437.3893; Found 1437.3876.

ATR-FTIR (cm^{-1}): 3068 (C-H stretch of aromatics), 2927 and 2852 (C-H stretch of alkane), 1701 (C=O stretch), 1498 (C-C stretch of aromatics), 1207 (C-N stretch), and 1043 (C-O stretch).

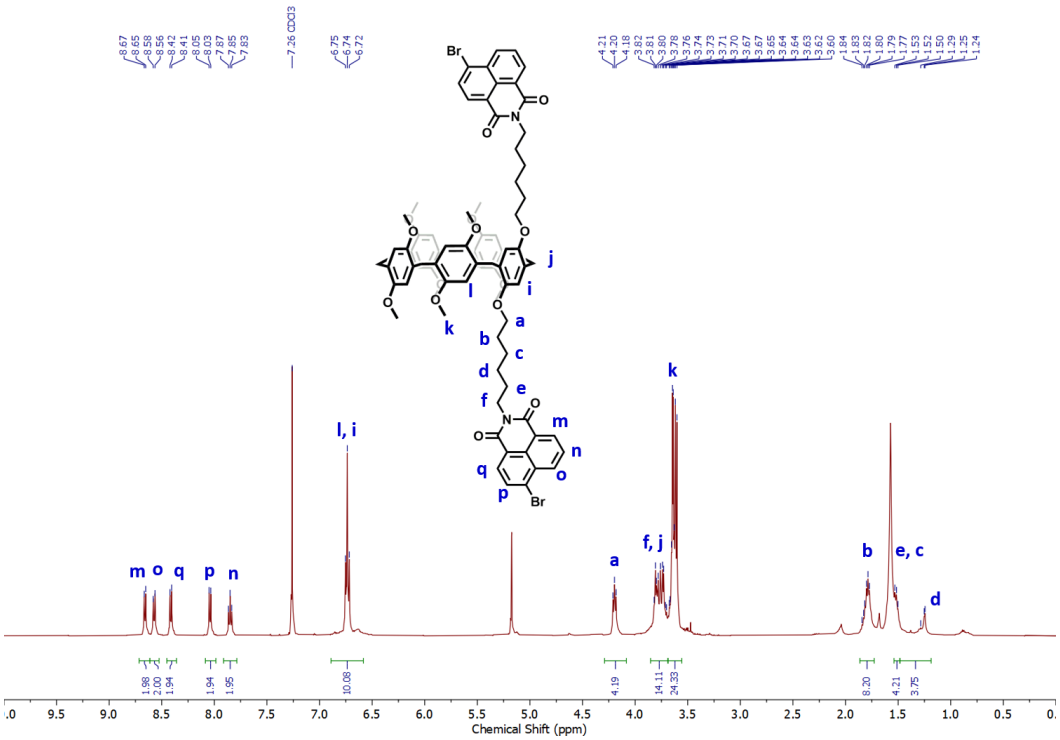

Figure S12 ^{1}H NMR spectrum (500 MHz, $CDCl_3$, 298 K) of **5**.

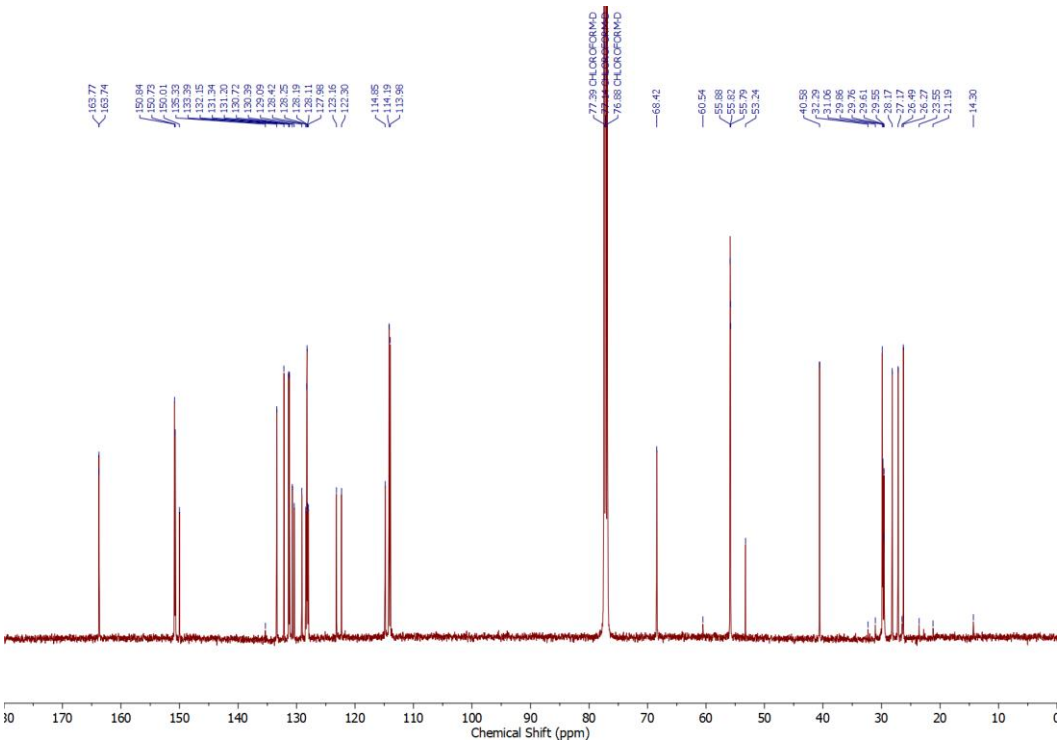

Figure S13 ^{13}C NMR spectrum (126 MHz, $CDCl_3$, 298 K) of **5**.

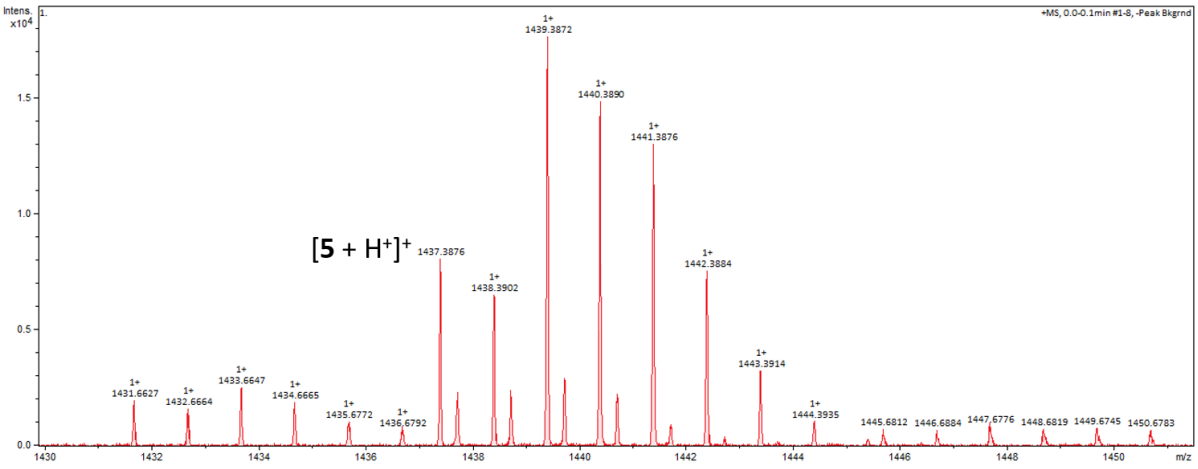

Figure S14 HRMS mass spectrum of **5**.

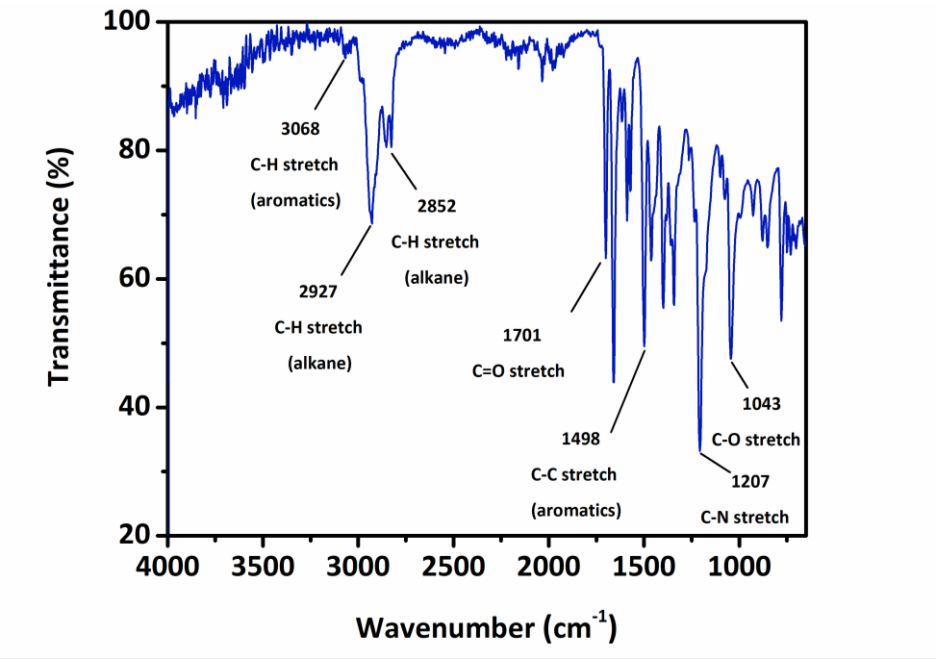

Figure S15 ATR-FTIR spectrum of **5**.

2.6 Synthesis of bis-hydrazide napthlimide copillar[5]arene (HNP5A)

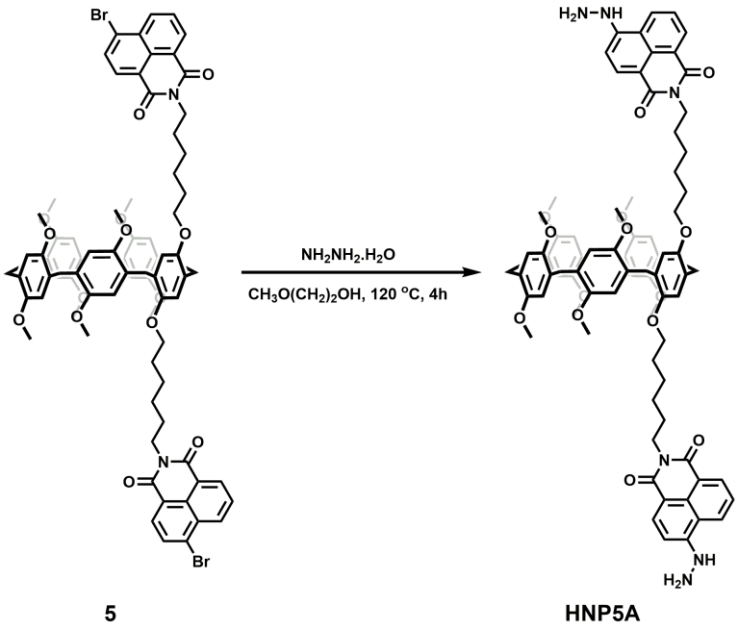

5 HNP5A

A product **5** (0.10 g, 0.07 mmol) was dissolved in 2-methoxyethanol (2.00 mL) and stirred under a nitrogen atmosphere at 120 °C for 10 minutes. Hydrazine monohydrate (0.17 mL, 3.47) was subsequently added and the solution was stirred for further 4 hours. After cooling to room temperature, the solution was washed with dichloromethane and deionized water several times. The organic layer was collected, then dried over anhydrous sodium sulfate, and the solvent was evaporated in vacuo to get the target product **HNP5A** as a yellow solid (quantitative yield).

^{1}H NMR [500 MHz, Acetone-d_6] δ 9.14 (s, 2H), 8.16 (d, *J* = 8.9 Hz, 2H), 8.57 (d, *J* = 7.4 Hz, 2H), 8.49 (d, *J* = 8.6 Hz, 2H), 7.75 (t, *J* = 7.9 Hz, 4H), 6.88 – 6.86 (m, 10H), 5.67 (s, 4H), 4.21 (t, *J* = 7.3 Hz, 4H), 3.97 – 3.85 (m, 4H), 3.74-3.73 (m, 34H), 1.94 – 1.88 (m, 4H), 1.87 – 1.81 (m, 4H), 1.74 – 1.67 (m, 4H), 1.61 – 1.57 (m, 4H).

^{13}C NMR [100 MHz, DMSO-d_6] δ 164.26, 163.91, 163.40, 153.57, 150.33, 150.27, 149.62, 134.64, 131.15, 131.02, 129.77, 128.70, 128.06, 128.00, 127.90, 127.87, 127.64, 124.60, 122.52, 122.22, 118.94, 114.52, 113.70, 107.94, 104.50, 74.35, 68.23, 60.48, 58.48, 55.85, 55.82, 55.77, 55.35, 29.57, 29.37, 28.14, 27.98, 26.98, 26.07.

DEPT 135 [100 MHz, DMSO-d_6] δ 134.74, 134.64, 131.15, 131.02, 128.70, 127.64, 124.59, 114.51, 113.68, 104.49, 74.35, 70.24, 68.22, 66.11, 60.47, 58.48, 55.84, 55.82, 55.76, 55.35, 39.61, 30.23, 29.57, 29.38, 28.14, 27.98, 26.98, 26.07, 11.28.

MALDI-TOF MS m/z: $[C_{79}H_{84}N_6O_{14}]^+$ calcd for 1340.6046; Found 1340.160, $[C_{79}H_{84}N_6O_{14} + 2H^+ + Na^+]^+$ calcd for 1365.6083; Found 1365.479, $[C_{79}H_{84}N_6O_{14} + H^+ + K^+]^+$ calcd for 1380.5750; Found 1380.479

HRMS (ESI) m/z: $[C_{79}H_{84}N_6O_{14} + 2H^+ + Na^+]^+$ calcd for 1365.6083; Found 1365.6045.

ATR-FTIR (cm^{-1}): 3369 (N-H stretch), 3066 (C-H stretch of aromatics), 2925 and 2852 (C-H stretch of alkane), 1699(C=O stretch), 1500 (C-C stretch of aromatics), 1207 (C-N stretch), and 1045 (C-O stretch).

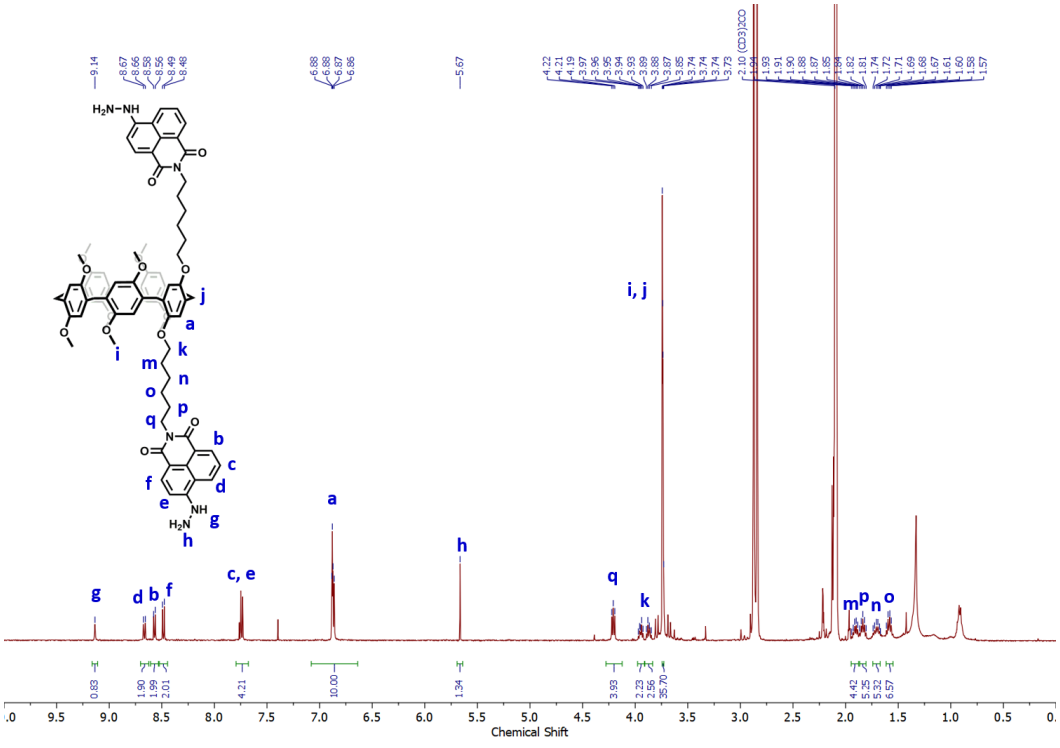

Figure S16 ^{1}H NMR spectrum (500 MHz, Acetone-d_6, 298 K) of **HNP5A**.

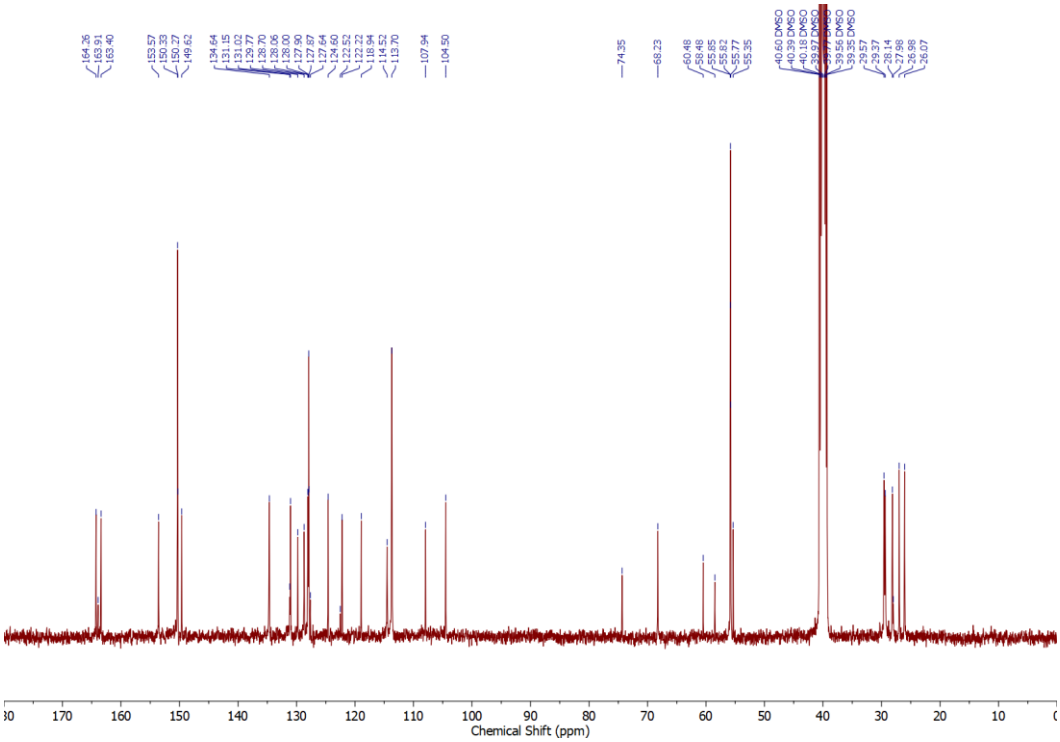

Figure S17 ^{1}C NMR spectrum (100 MHz, DMSO-d_6, 298 K) of **HNP5A**.

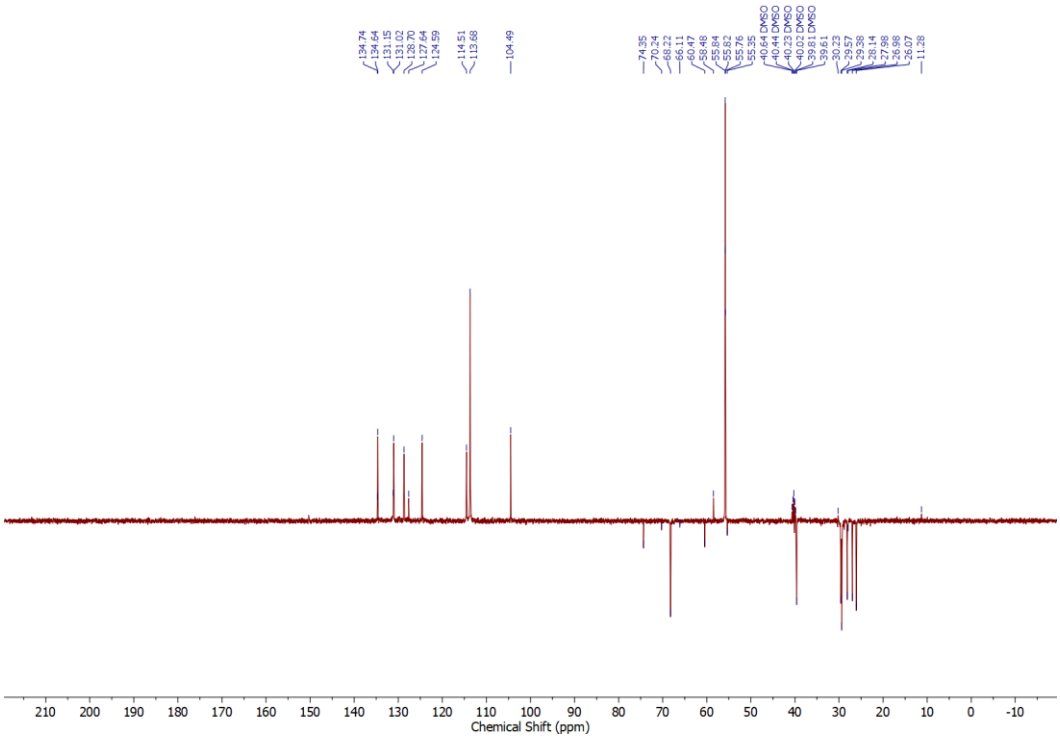

Figure S18 DEPT 135 spectrum (400 MHz, DMSO-d_6, 298 K) of **HNP5A**.

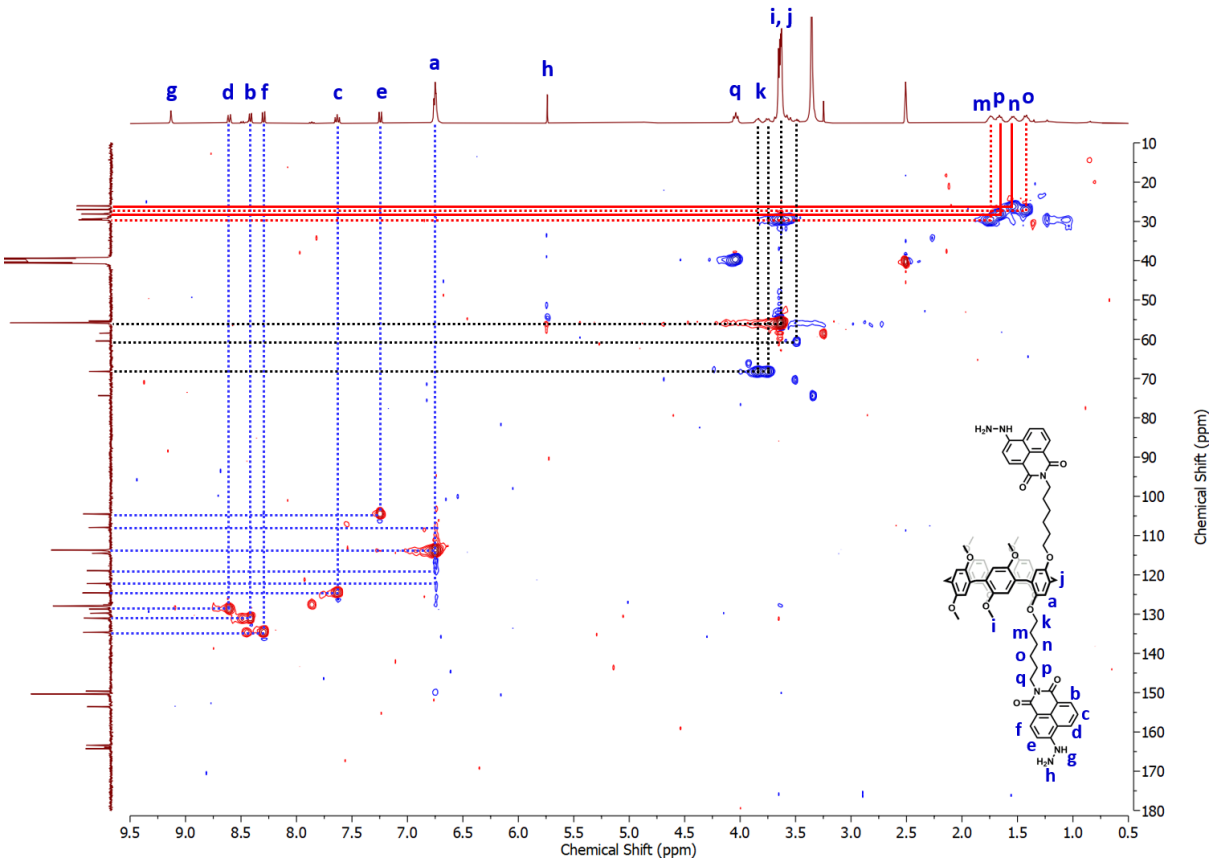

Figure S19 HSQC spectrum (400 MHz, DMSO-d_6, 298 K) of **HNP5A**.

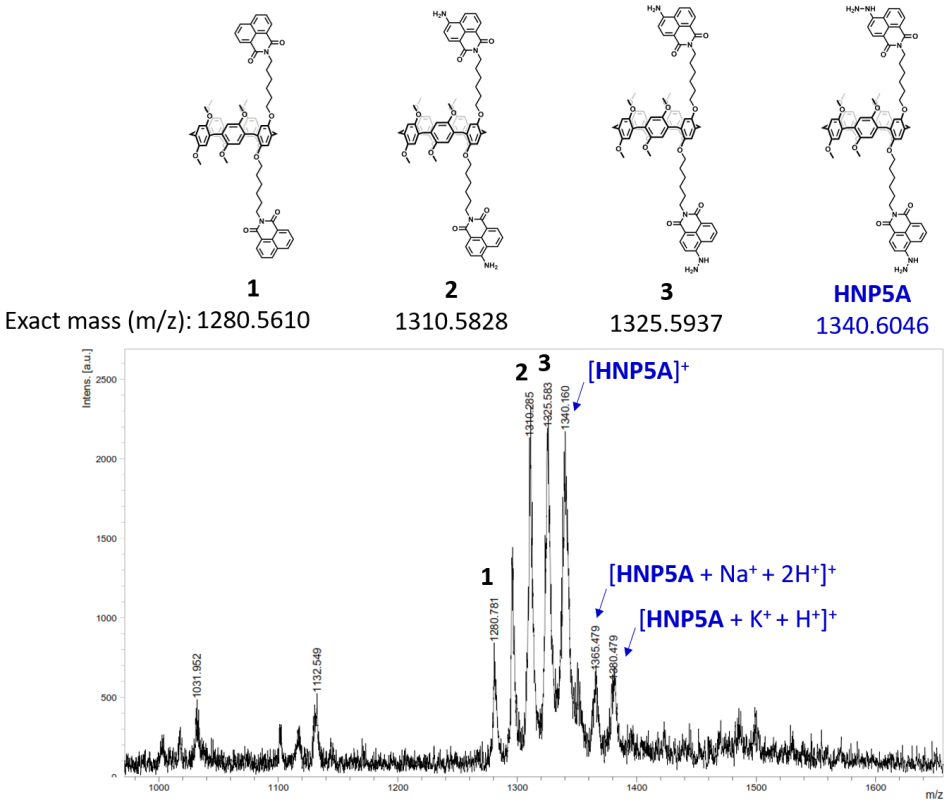

Figure S20 MALDI-TOF mass spectrum of **HNP5A**.

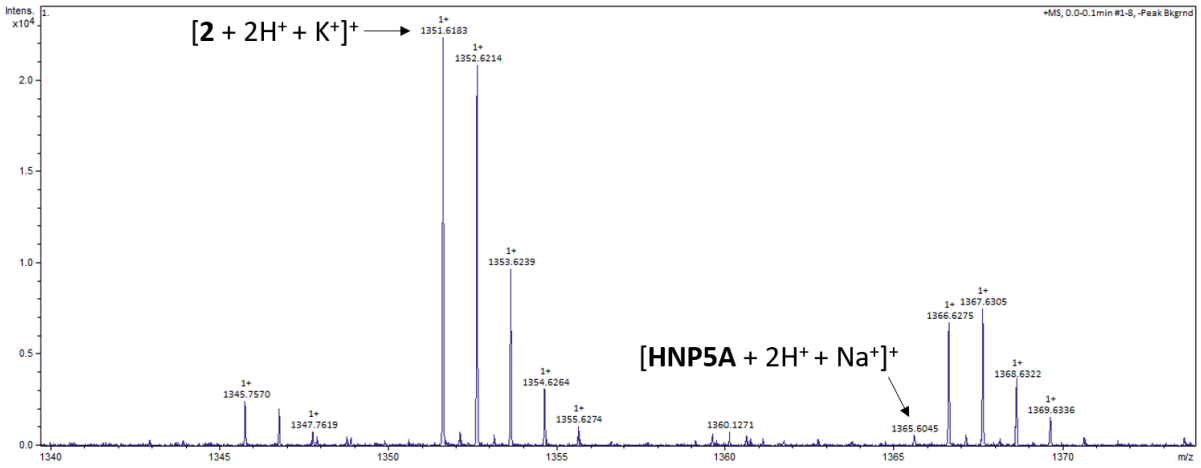

Figure S21 HRMS-ESI mass spectrum of **HNP5A**.

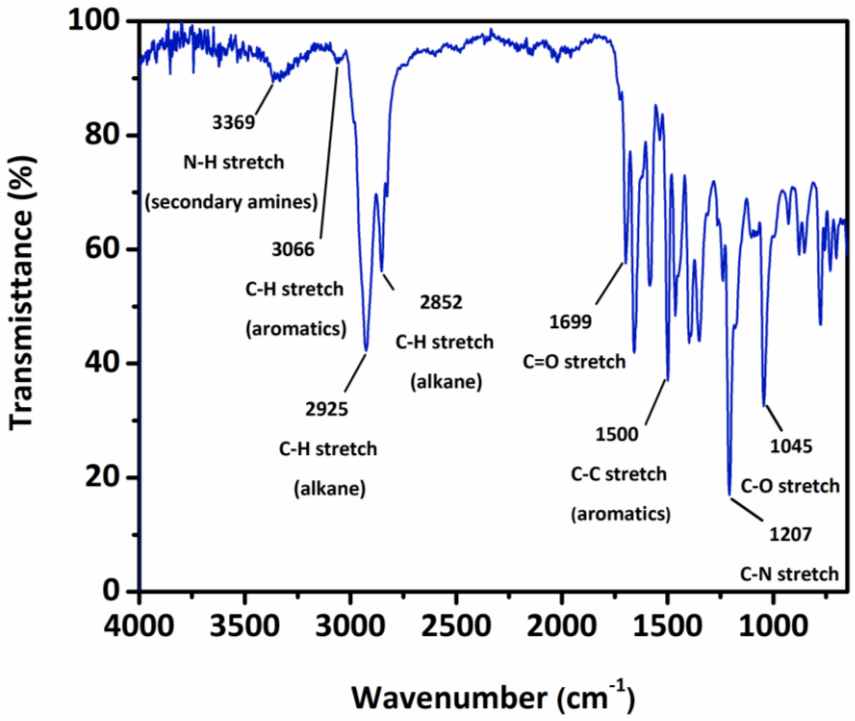

Figure S22 ATR-FTIR spectrum of **HNP5A**.

2.7 Solvent variation for characterization of HNP5A

Each sample was prepared in an NMR tube containing 1×10^{-3} M **HNP5A** in various deuterated solvents such as a mixture of 1:1 MeOD:$CDCl_3$, CD_3CN-d_3, acetone-d_6, and DMSO-d_6.

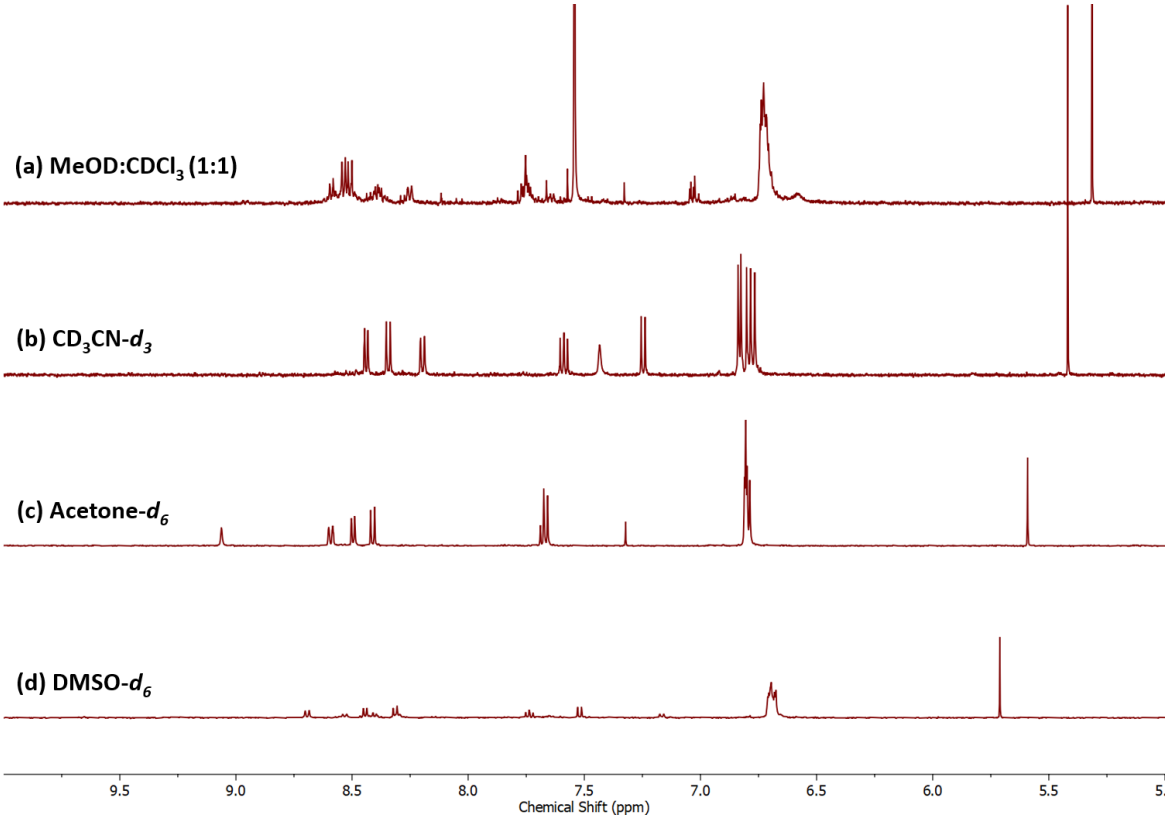

Figure S23 ^{1}H NMR spectrum (500 MHz, 298 K) of 1 mM **HNP5A** in various solvents.

3. Synthesis and characterization of fluorescence probe HNOB

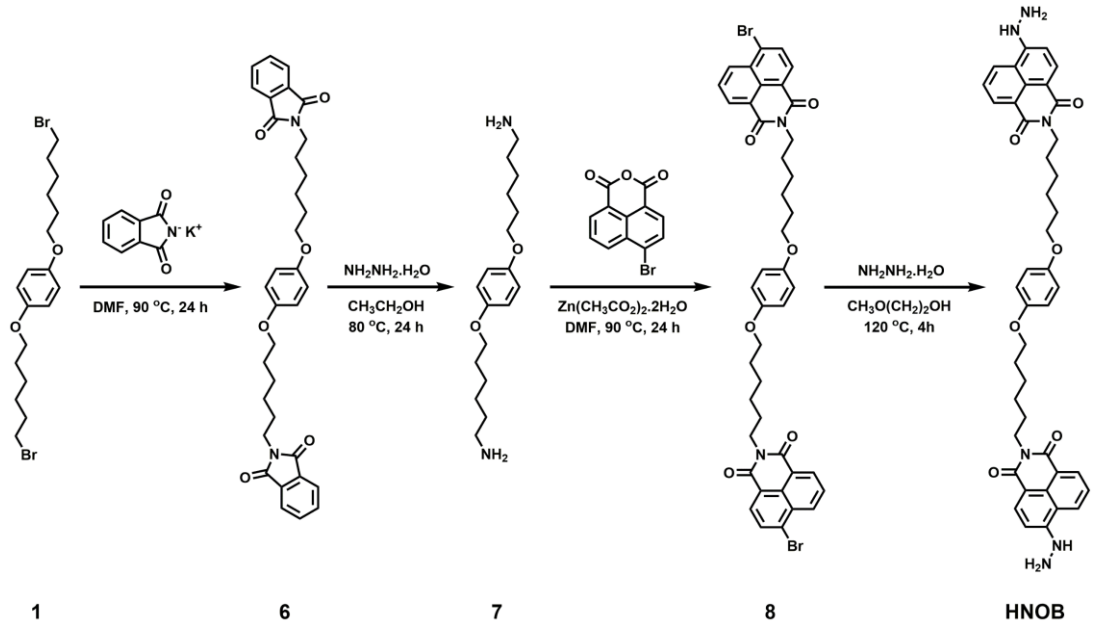

Figure S24 Synthesis pathway of **HNOB**.

3.1 Synthesis of 6

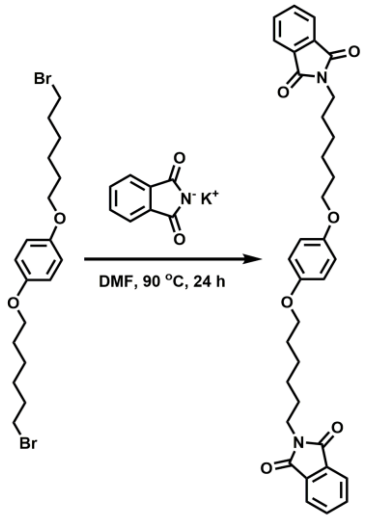

1 **6**

A mixture of **1** (1.00 g, 2.29 mmol) and potassium phthalimide (1.27 g, 6.88 mmol) was dissolved in dimethylformamide (4.00 mL). The suspension was refluxed at 90 °C for 24 hours. After cooling to room temperature, the dimethylformamide was evaporated following adding of toluene and chloroform, respectively. The crude product was extracted with ethyl acetate and deionized water several times and brine last time, then dried over anhydrous sodium sulfate. The solvent was removed under reduced pressure to receive product **6** as a white solid (quantitative yield).

^{1}H NMR [500 MHz, $CDCl_3$] δ 7.84 (dd, *J* = 5.3, 2.8 Hz, 4H), 7.71 (dd, *J* = 5.5, 3.0 Hz, 4H), 6.78 (s, 4H), 3.88 (t, *J* = 7.5 Hz, 4H), 3.69 (t, *J* = 7.5 Hz, 4H), 1.77 – 1.67 (m, 8H), 1.52 – 1.46 (m, 4H), 1.43 – 1.37 (m, 4H).

^{13}C NMR (126 MHz, $CDCl_3$) δ 168.60, 168.04, 153.17, 134.43, 133.98, 132.72, 132.22, 123.70, 123.29, 115.43, 77.40, 77.14, 76.89, 68.45, 38.04, 29.80, 29.31, 28.65, 26.74, 26.51, 25.79.

HRMS (ESI) m/z: $[C_{34}H_{36}N_2O_6 + Na^+]^+$ calcd for 591.2466; Found 591.2484.

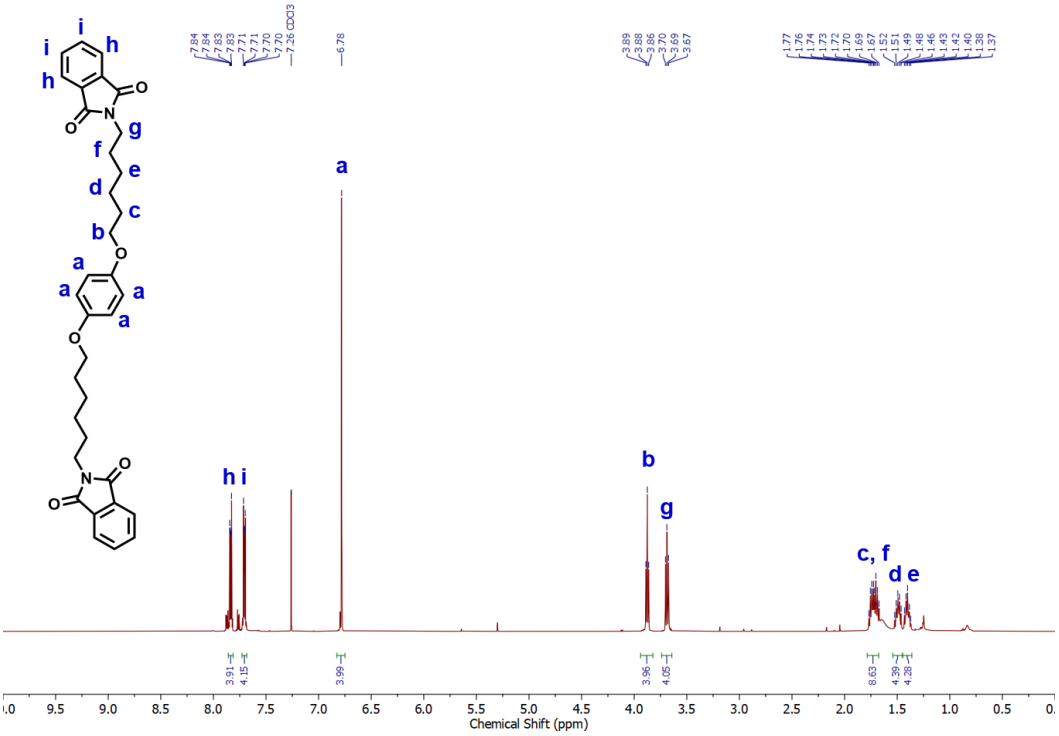

Figure S25 ^{1}H NMR spectrum (500 MHz, $CDCl_3$, 298 K) of **6**.

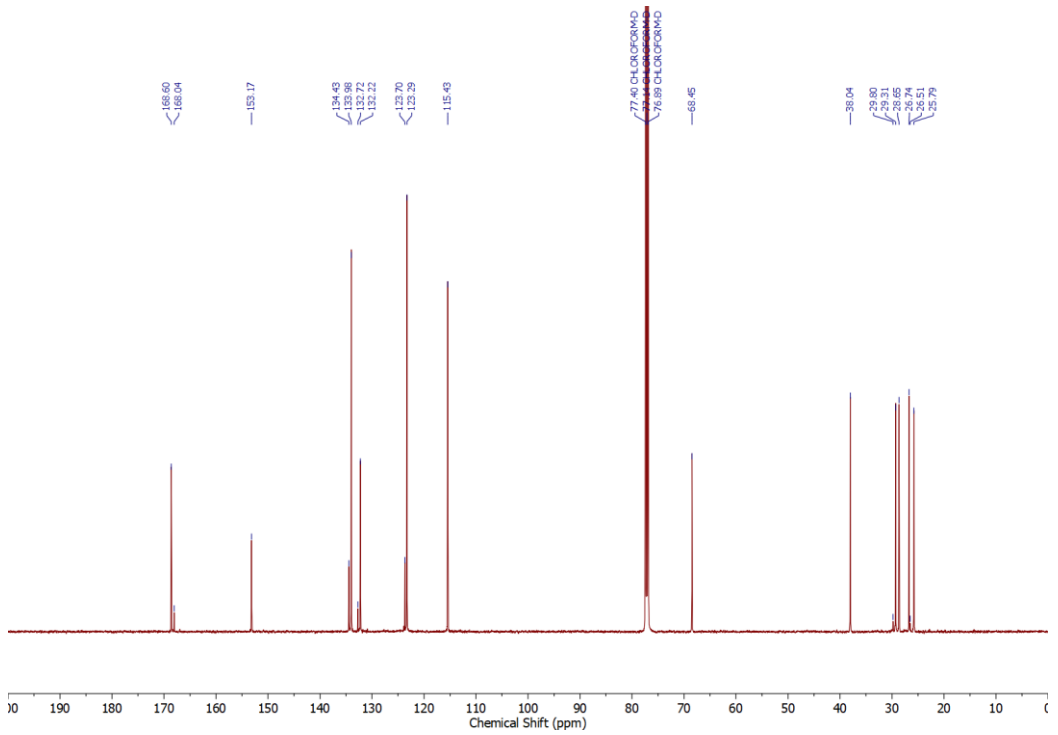

Figure S26 ^{13}C NMR spectrum (126 MHz, $CDCl_3$, 298 K) of **6**.

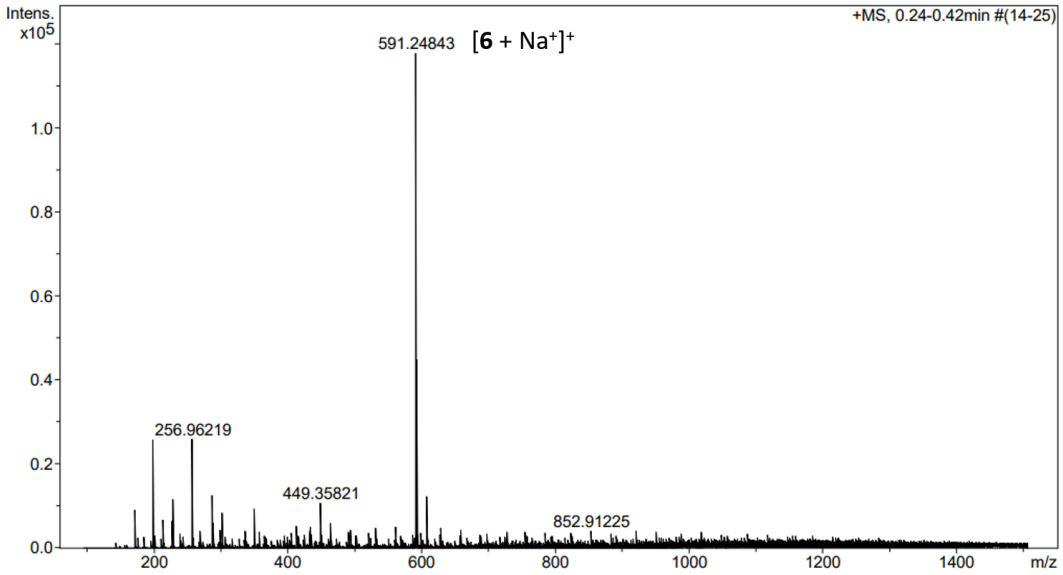

Figure S27 HRMS-ESI mass spectrum of **6**.

3.2 Synthesis of bis-amino oxybenzene (7)

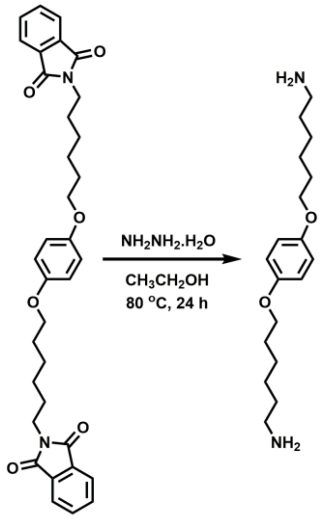

6 **7**

Product **6** (1.27 g, 2.24 mmol) was dissolved in ethanol (50 mL) under nitrogen gas. Hydrazine monohydrate (2.18 mL, 44.84 mmol) was subsequently added to produce a white solid and the suspension was stirred at 90 °C overnight. The mixture solution was evaporated to remove hydrazine and ethanol. The crude product was dissolved in dichloromethane and washed with deionized water (3 × 100.00 mL), then dried over anhydrous sodium sulfate, and the solvent was removed under reduced pressure to obtain product **7** as a white solid (0.55 g, 79.4% yield)

^{1}H NMR [500 MHz, DMSO-d_6] δ 6.82 (s, 4H), 3.87 (t, J = 7.5 Hz, 4H), 1.69 – 1.63 (m, 4H), 1.41 – 1.27 (m, 16H).

^{13}C NMR [126 MHz, DMSO-d_6] δ 153.12, 115.74, 68.28, 61.16, 42.20, 33.95, 33.04, 29.39, 26.76, 26.06.

HRMS (ESI) m/z: $[C_{18}H_{32}N_2O_2 + Na^+ + (CH_3)_2O]^+$ Calcd for 389.2775; Found 389.3189

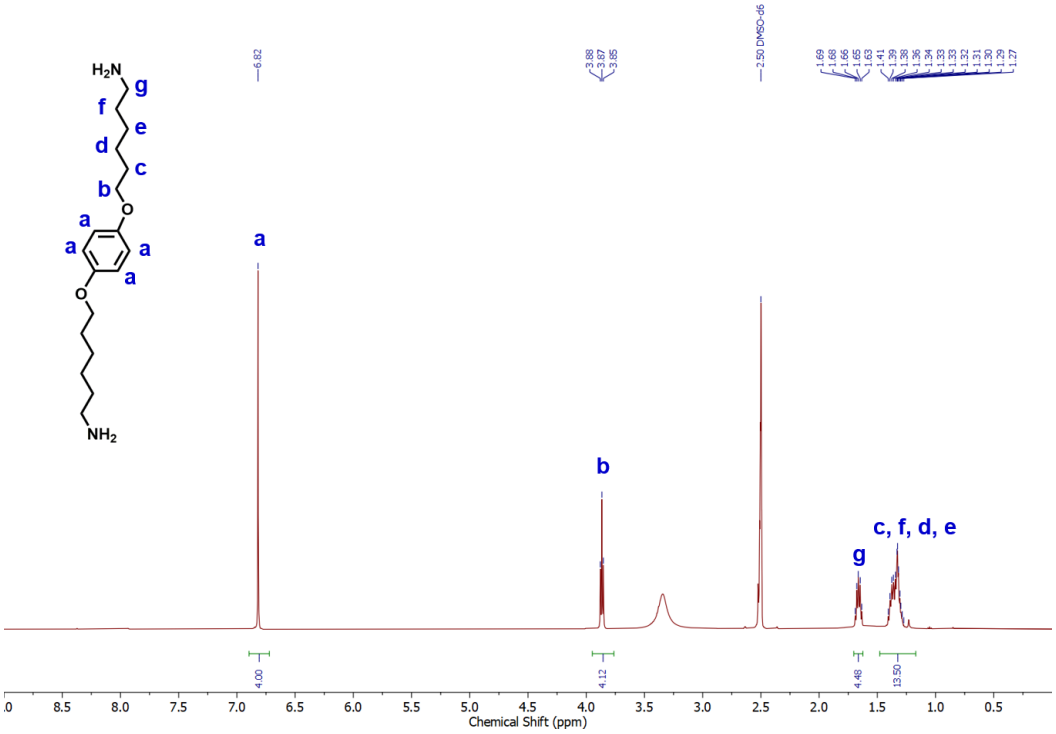

Figure S28 ^{1}H NMR spectrum (500 MHz, $CDCl_3$, 298 K) of **7**.

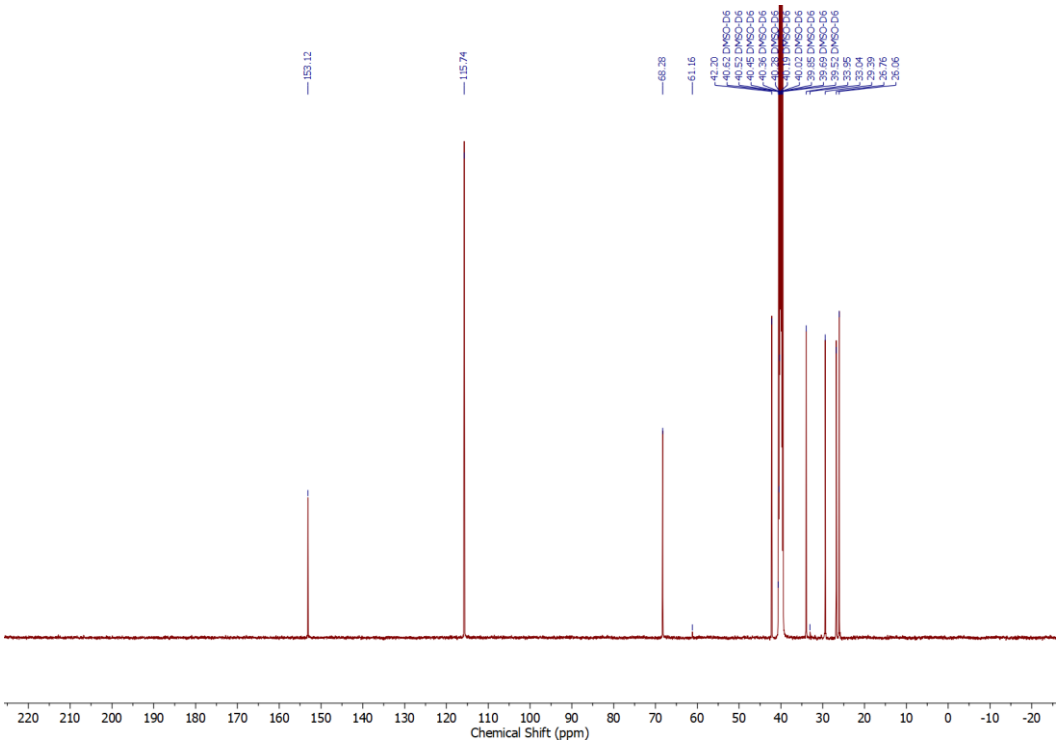

Figure S29 ^{13}C NMR spectrum (500 MHz, $CDCl_3$, 298 K) of **7**.

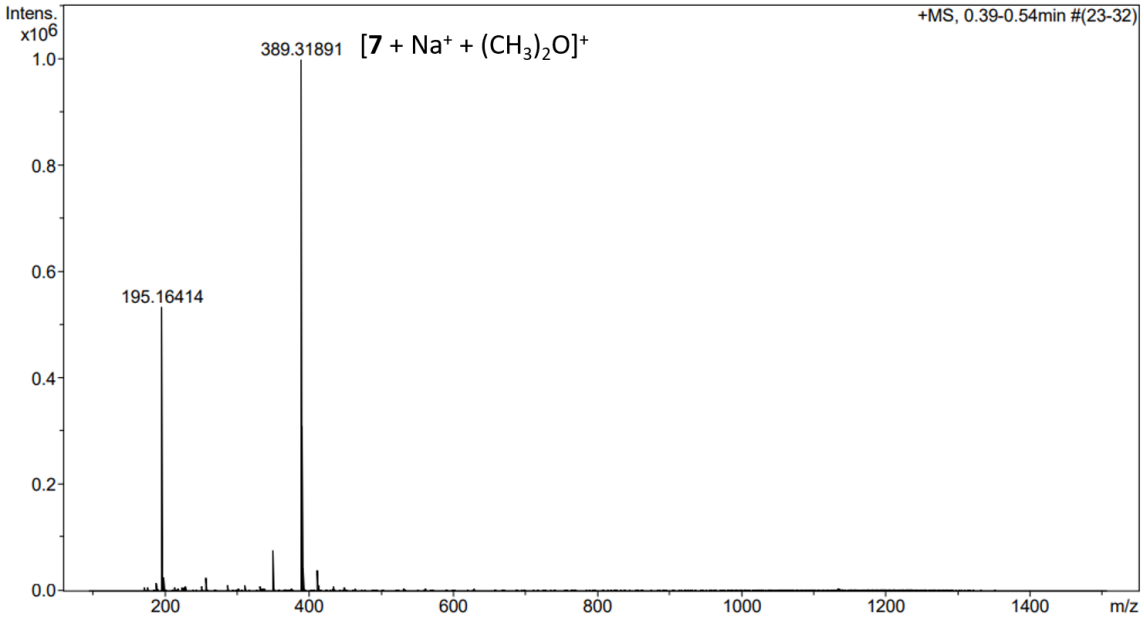

Figure S30 HRMS-ESI mass spectrum of **7**.

3.3 Synthesis of bis-bromo napthlimide copillar[5]arene (8)

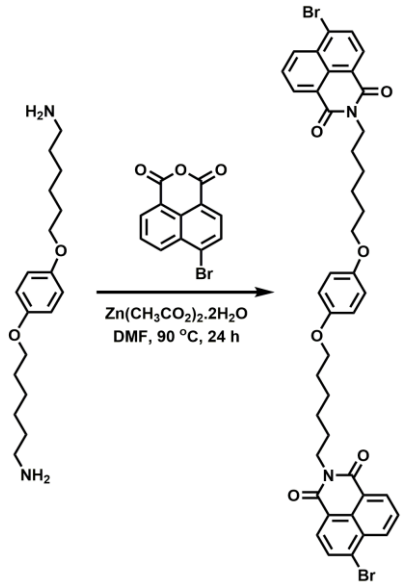

7 **8**

A mixture of product **7** (0.46 g, 1.50 mmol), 4-bromo-1,8-naphthalic anhydride (1.25 g, 4.49 mmol), and zinc acetate dihydrate with a catalyst amount was dissolved in DMF (4.00 mL). The reaction solution was refluxed at 90 °C under nitrogen for 24 hours. After the complete reaction, the mixture solution was left out to room temperature and ethanol was added into the solution to precipitate. Then, the precipitate was filtrated and washed with ethanol. The precipitate was recrystallized with dichloromethane and ethanol, respectively. Lastly, the precipitate was filtrated and washed with ethanol to acquire product **8** as a pale-yellow solid (0.62 g, 50.2% yield).

^{1}H NMR [500 MHz, $CDCl_3$] δ 8.65 (dd, *J* = 7.3, 1.1 Hz, 2H), 8.57 (dd, *J* = 8.5, 1.1 Hz, 2H), 8.41 (d, *J* = 7.9 Hz, 2H), 8.04 (d, *J* = 7.9 Hz, 2H), 7.85 (dd, *J* = 8.5, 7.3 Hz, 2H), 6.78 (s, 4H), 4.18 (t, *J* = 7.5 Hz, 4H), 3.88 (t, *J* = 6.5 Hz, 4H), 1.79 – 1.73 (m, 8H), 1.56 – 1.45 (m, 8H).

^{13}C NMR [126 MHz, $CDCl_3$] δ 163.78, 153.21, 133.41, 132.20, 131.40, 131.24, 130.77, 130.39, 129.15, 128.24, 123.25, 122.39, 115.45, 68.54, 53.59, 40.61, 31.11, 29.38, 28.13, 26.99, 25.96.

HRMS (ESI) m/z: $[C_{42}H_{38}Br_2N_6O_6 + Na^+]^+$ calcd for 847.0989; Found 847.1008.

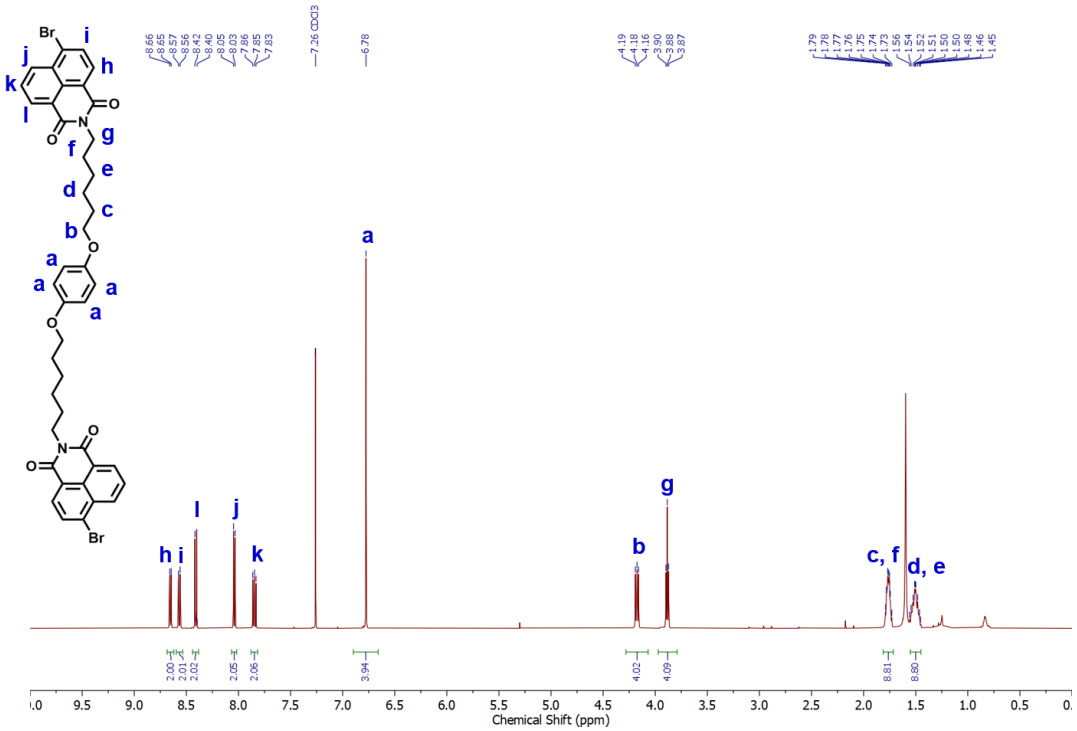

Figure S31 ^{1}H NMR spectrum (500 MHz, $CDCl_3$, 298 K) of **8**.

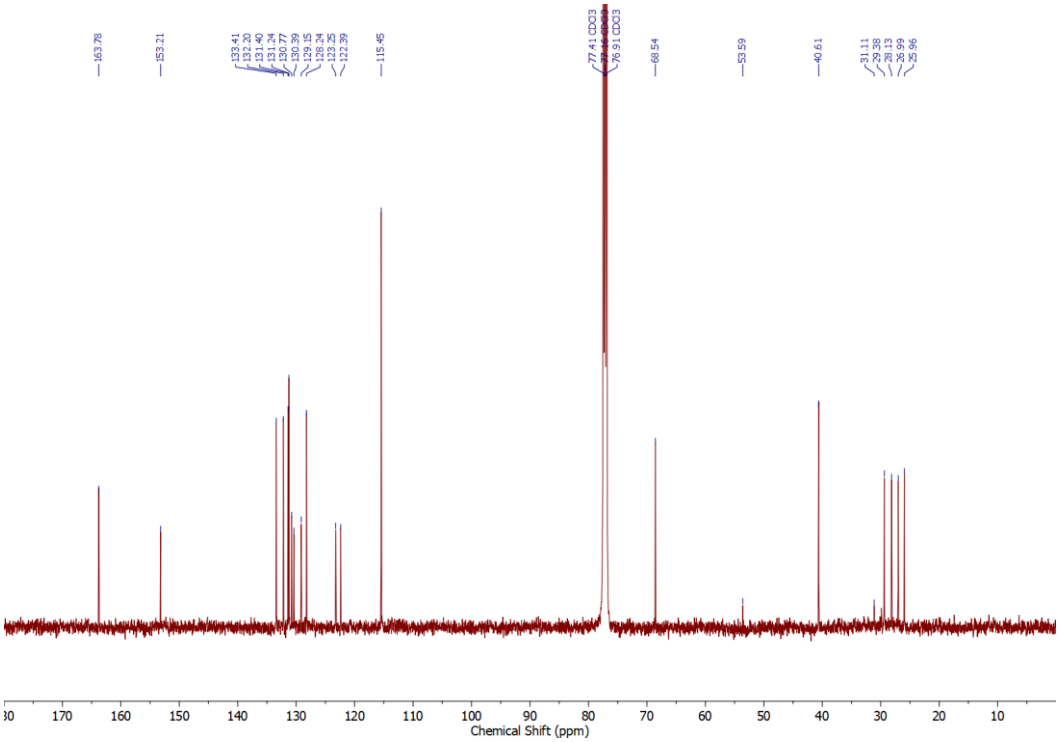

Figure S32 ^{13}C NMR spectrum (126 MHz, $CDCl_3$, 298 K) of **8**.

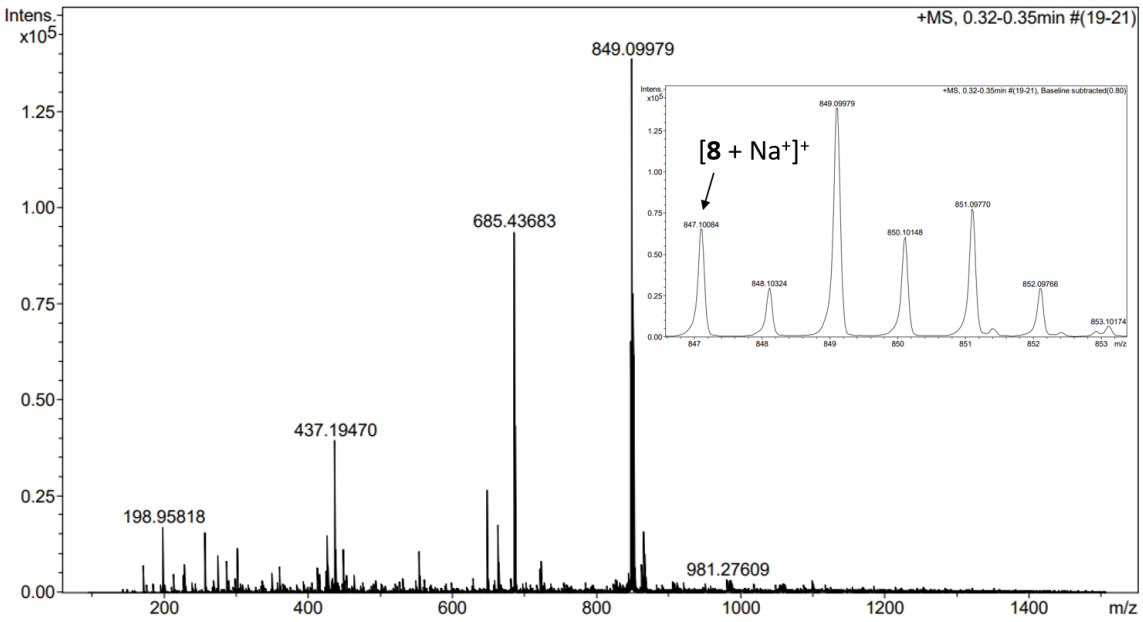

Figure S33 HRMS-ESI mass spectrum of **8**.

3.4 Synthesis and characterization of bis-hydrazine napthalimide oxybenzene (HNOB)

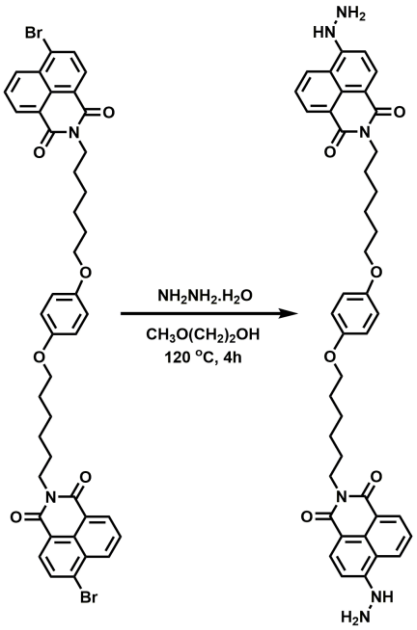

8 **HNOB**

Product **8** (0.051 g, 0.0617 mmol) was dissolved in 2-methoxyethanol (2.00 mL) and stirred under a nitrogen atmosphere at 120 °C for 10 minutes. Hydrazine monohydrate (0.15 mL, 3.085 mmol) was subsequently added and the solution was stirred for further 4 hours. The product was precipitated in the reaction. After cooling to room temperature, the precipitate was filtrated and washed with ethanol to receive the product **HNOB** as a yellowish-orange solid (0.04 g, 78.4% yield).

^{1}H NMR [500 MHz, DMSO-d_6] δ 9.10 (s, 2H), 8.57 (dd, *J* = 8.7, 1.3 Hz, 2H), 8.37 (dd, *J* = 7.4, 1.1 Hz, 2H), 8.25 (d, *J* = 8.6 Hz, 2H), 7.59 (dd, *J* = 8.4, 7.3 Hz, 2H), 7.20 (d, *J* = 8.6 Hz, 2H), 6.74 – 6.73 (m, 4H), 4.65 (s, 4H), 3.97 (t, *J* = 5.2 Hz, 4H), 3.82 (t, *J* = 6.5 Hz, 4H), 1.66 – 1.55 (m, 8H), 1.47 – 1.28 (m, 8H).

^{13}C NMR [126 MHz, DMSO-d_6] δ 164.31, 163.45, 153.72, 153.07, 134.78, 131.15, 129.84, 128.79, 124.69, 122.28, 118.97, 115.70, 107.88, 104.55, 68.25, 29.18, 28.15, 26.87, 25.88.

HRMS (ESI) m/z: $[C_{42}H_{44}N_6O_6 + 2Na^+ + (CH_3)_2O]^+$ calcd for 832.3525; Found 832.3883.

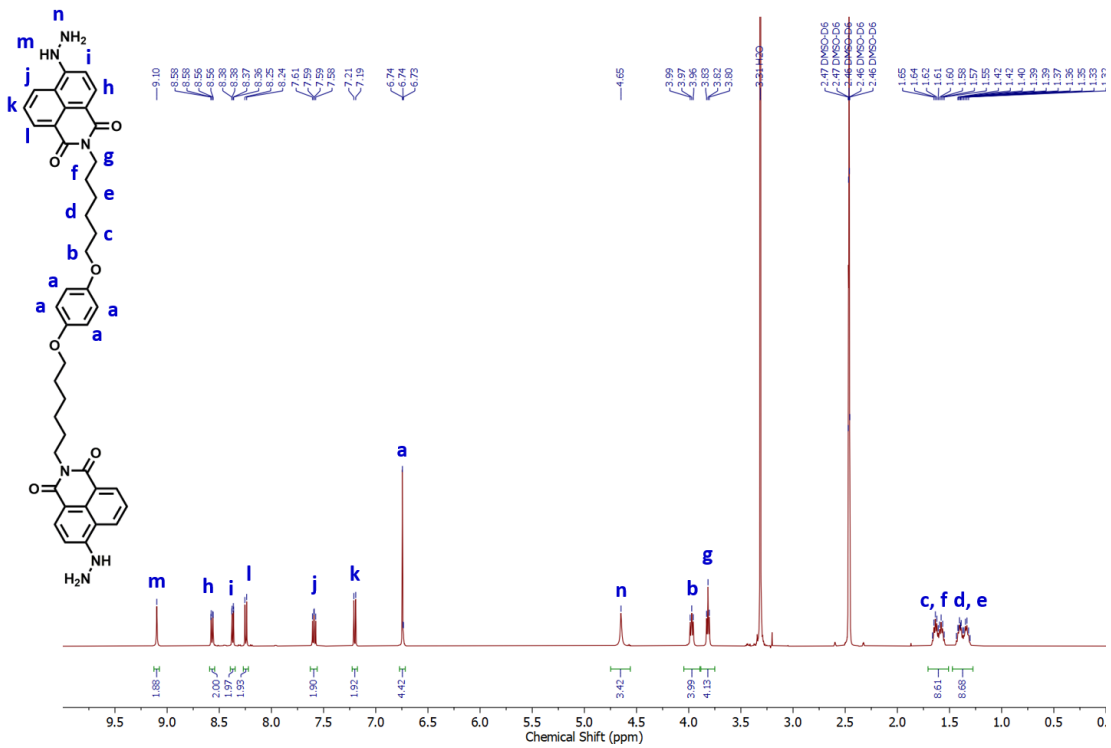

Figure S34 ^{1}H NMR spectrum (500 MHz, $CDCl_3$, 298 K) of **HNOB**.

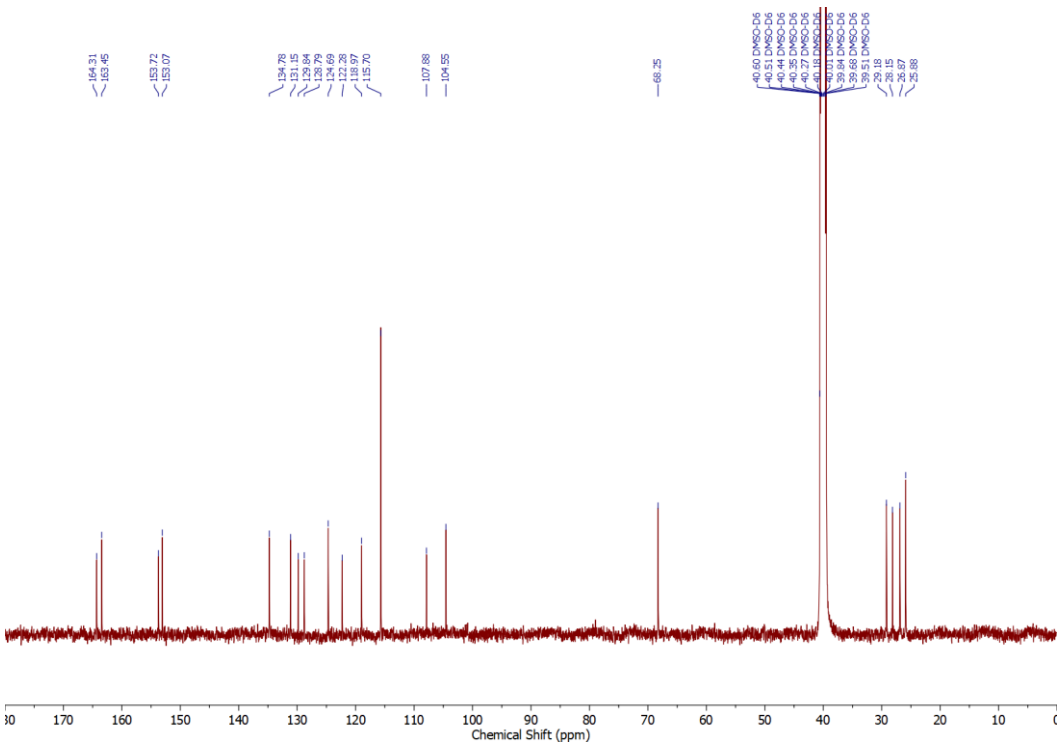

Figure S35 ^{13}C NMR spectrum (126 MHz, $CDCl_3$, 298 K) of **HNOB**.

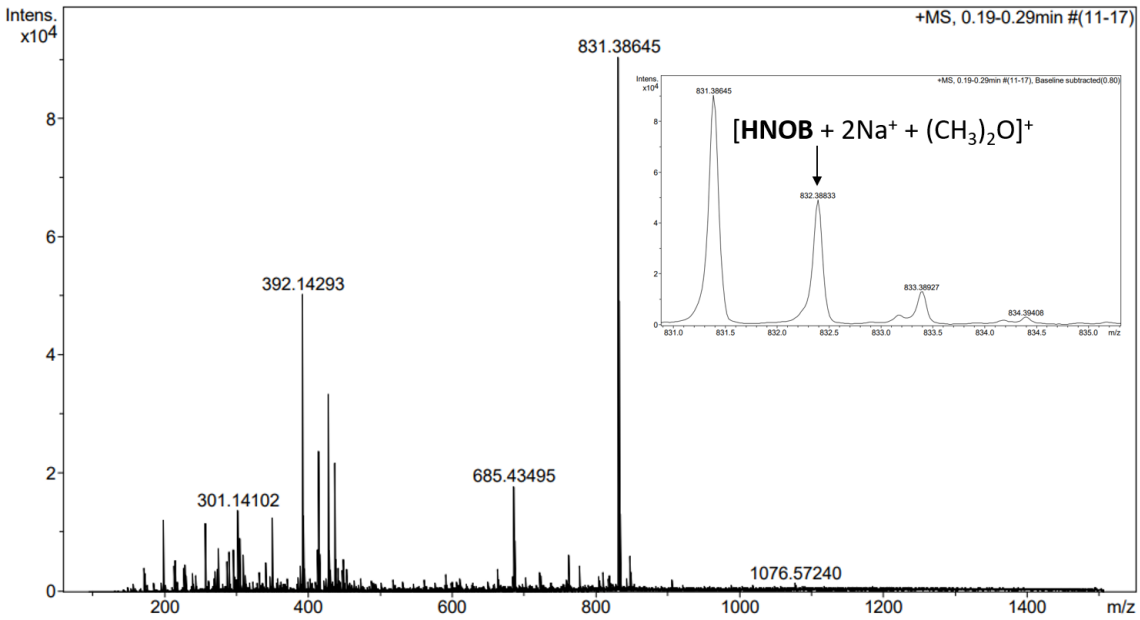

Figure S36 HRMS-ESI mass spectrum of **HNOB**.

4. Host-guest complexation studies of HNP5A⊂C9 in DMSO-d_6 by ^{1}H NMR titration, 2D NOESY NMR and HRMS (ESI) techniques

4.1 ^{1}H NMR titration

A 2 mM **HNP5A** solution was prepared in DMSO-d_6 and a portion of 0.5 mL was transferred into an NMR tube covered with a plastic cap. A 2 µL of trifluoroacetic acid as a catalyst was subsequently added to the solution. A divided **C9** solution was also prepared at 100 mM in DMSO-d_6 containing a small vial and added in aliquots. The mixture solution was shaken before ^{1}H NMR spectra were recorded at 0.0, 1.0, 2.0, 3.0 equivalents of **C9**, 3, 10, and 15 minutes of reaction time.

4.2 HRMS and 2D-NOESY NMR techniques

To prepare the complexation, a 4 mM **HNP5A** solution was dissolved in DMSO-d_6 and a portion of 0.5 mL was transferred into an NMR tube covered with a plastic cap. A 2 µL of trifluoroacetic acid as a catalyst was subsequently added to the solution. A 200 mM **C9** solution was also prepared in DMSO-d_6 containing a small vial and added 30 µL or 3.0 equivalents into the solution. The sample was shaken and left out for 15 minutes before spectra were recorded.

HRMS (ESI) m/z: $[C_{97}H_{116}N_6O_{14} + H^+]^+$ calcd for 1589.8622; Found 1589.8611.

$[C_{97}H_{116}N_6O_{14} + H^+ + Na^+]^+$ calcd for 1612.8515; Found 1612.8399.

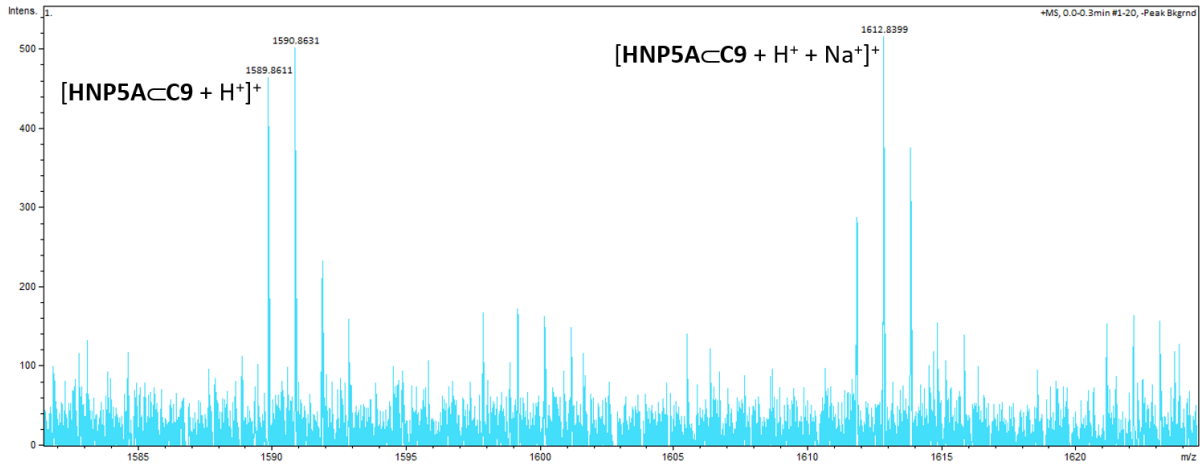

Figure S37 HRMS-ESI (DMSO-d_6) spectrum of 1:3 mixture of **HNP5A** and **C9** using trifluoroacetic acid (TFA) as a catalyst.

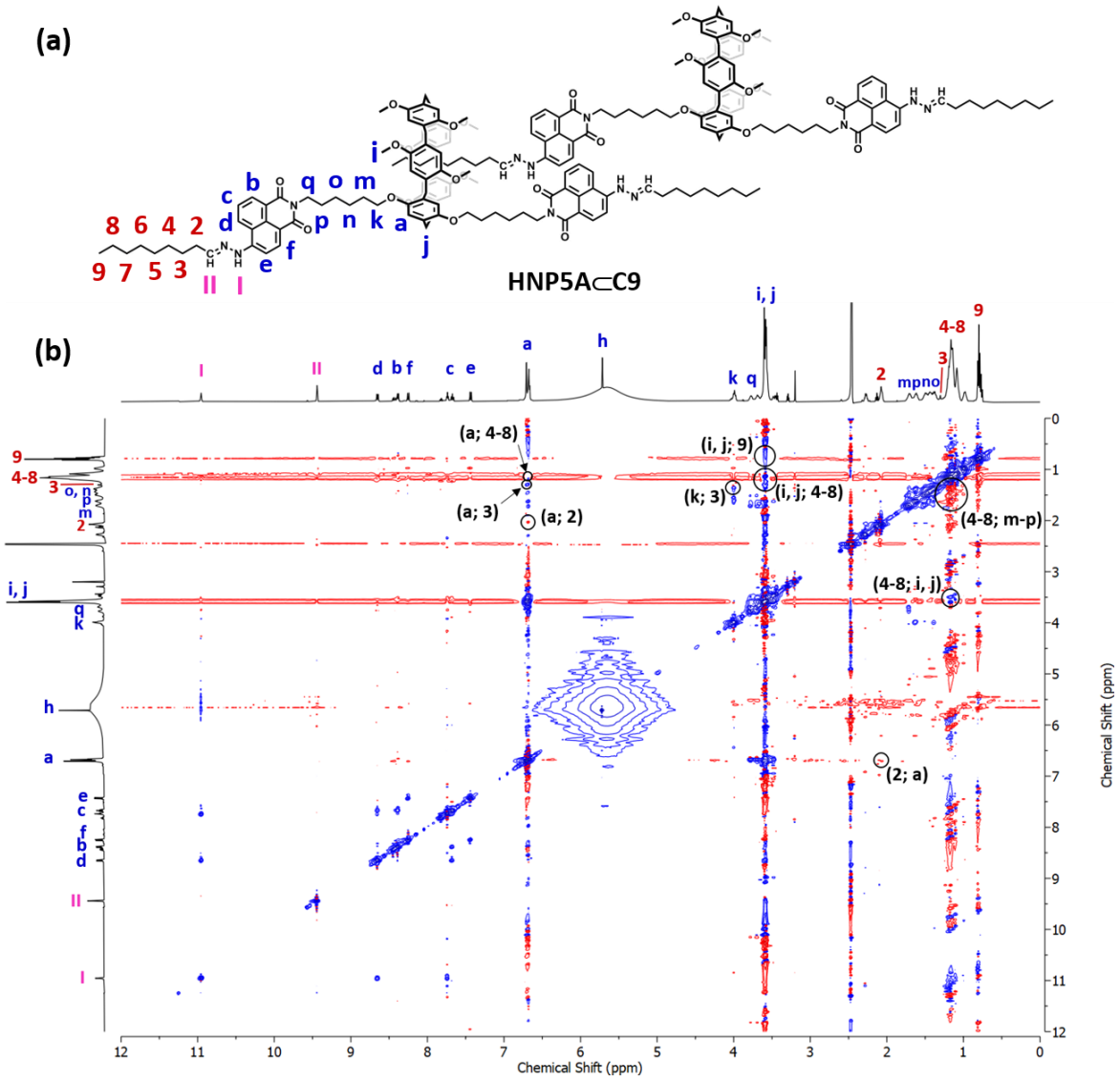

Figure S38 (a) Chemical structure of complex **HNP5A⊂C9** and (b) 2D NOESY (DMSO-d_6) NMR spectrum of 1:3 mixture of **HNP5A** and **C9** using trifluoroacetic acid (TFA) as a catalyst.

4.3 Solvent ratio optimization for guests detection procedure by fluorescence spectrophotometry

To optimize the solvent ratio, all samples were prepared in a quartz cuvette containing 1×10^{-5} M **HNP5A** in various ratios of DMSO/acetate buffer (0.01 M, pH 4) solution ranging from 100% to 5%. A 60 µL of 0.2 mM **HNP5A** was diluted with different volumes of DMSO from 2,850, 2,550, 2,250, 1,950, 1,650, 1,350, 1,050, 750, 450, 150, and 0 µL. Each portion was then adjusted with acetate buffer (0.01 M, pH 4) to obtain 3 mL of the final volume. Both the fluorescence spectra were recorded using fluorescence spectrophotometry and the naked-eye study was captured under UV light with a wavelength of 365 nm, respectively.

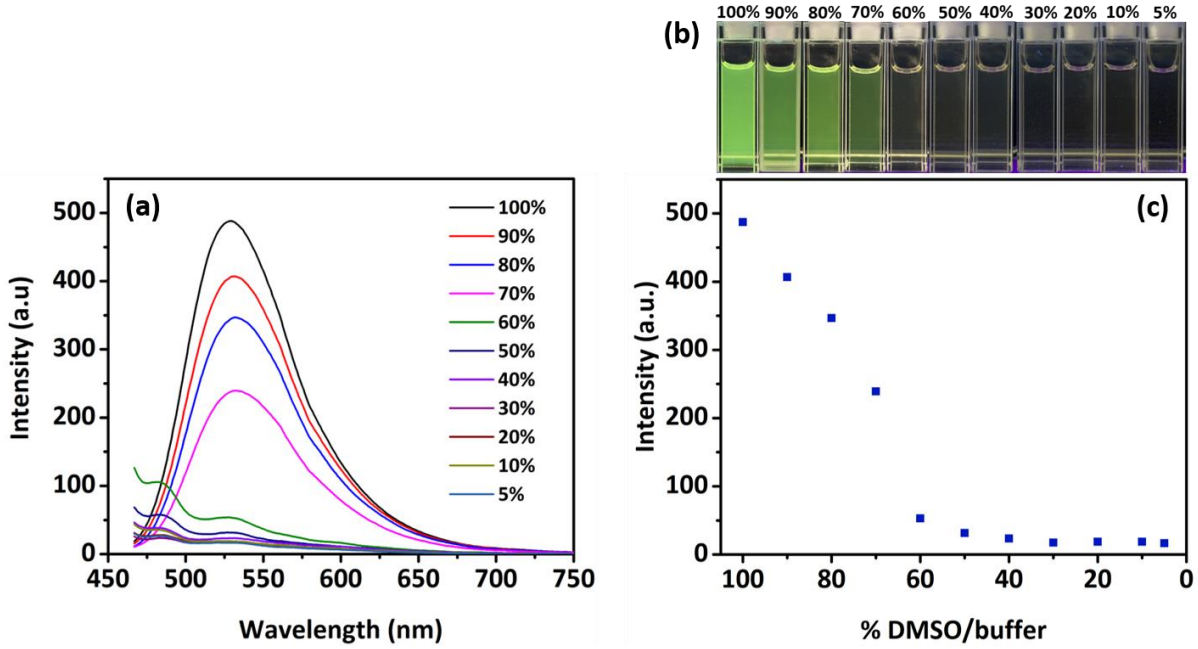

Figure S39 (a) Fluorescence spectra, (b) fluorescence intensities at 530 nm, and (c) visual fluorescence of **HNP5A-C9** in the different ratios of DMSO/0.01 M, pH 4 acetate buffer solution (λ_{ex} = 438 nm, PMT 590 V, slit width 10 nm).

According to fluorescence spectra, the intensity was dramatically decreased when the ratio of DMSO was decreased from 100% to 5% because of fluorescence quenching from water molecules. This result conformed to visual fluorescence which showed light green fluorescence to non-fluorescence after decreasing DMSO ratio. Since the concept of this work was designed to turn on fluorescence, the free probe **HNP5A** in media must give the lowest fluorescence emission. So, the optimum condition of the solvent ratio was 10% v/v DMSO/acetate buffer (0.01 M, pH 4) and the **HNP5A** dissolved clearly in this system.

5. pH and time variation for guests detection procedure by fluorescence spectrophotometry

To prepare each sample containing a quartz cuvette, a 60 µL of 0.1 M **C9** (2 mM) was added into the diluted solution of 150 µL of 0.2 mM **HNP5A** (1×10^{-5} M), 90 µL DMSO, and 2,700 µL of 0.01 M buffer with different pH at 3, 4, 5, and 6 to get 3 mL total volume. According to the pH range depending on buffer type, the citrate buffer was prepared to pH 3 and pH 6 while the acetate buffer

was prepared to pH 4 and pH 5. The mixture solution was subsequently stirred from 0 to 60 minutes. The fluorescence spectra were recorded for every reaction time variation.

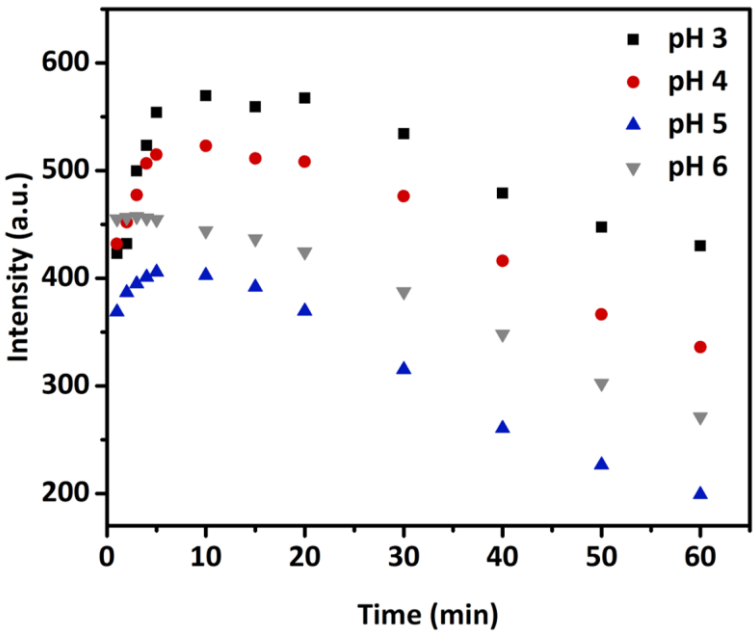

Figure S40 Fluorescence intensities at 530 nm of **HNP5A⊂C9** complex in 10% v/v DMSO/0.01 M with different pH of buffer and reaction time. (λ_{ex} = 438 nm, PMT 590 V, slit width 10 nm).

In accordance with the fluorescence intensity of complex **HNP5A⊂C9**, the intensities at pH 3, 4, and 5 were increased from 1 to 10 minutes and fluctuated until 15 minutes after that they were decreased continuously until 60 minutes. Whereas at pH 6, the intensities were steady for the first five minutes and then started to decline. Among various pH at 15 minutes, the intensity showed the highest peak at pH 3; however, the conditions of pH 4 with 15 minutes of reaction time were selected because complex **HNP5A⊂C9** could not sense metal ions in acidic solution at pH 3 for the following step. Therefore, the suitable complexation conditions were pH 4 and 15 minutes of reaction time.

6. Selectivity study of HNP5A towards various aldehyde compounds by fluorescence spectrophotometry

To prepare each portion, 150 µL of 0.2 mM **HNP5A** (1×10^{-5} M), 90 µL DMSO, and 2,700 µL of 0.01 M, pH 4 acetate buffer were mixed in a quartz cuvette. Then, a 60 µL of 0.1 M (2 mM) of various aldehyde compounds including formaldehyde (**C1**), propionaldehyde (**C3**), butyraldehyde (**C4**), valeraldehyde (**C5**), hexanal (**C6**), heptanal (**C7**), octanal (**C8**), and nonanal (**C9**) were added to the **HNP5A** solution to obtain 3 mL final volume. To complete the reaction, the mixture solution was vigorously stirred for 15 minutes. The fluorescence spectra were recorded and the visual fluorescence was also recorded under a wavelength of 365 nm UV light.

7. Sensitivity study of HNP5A towards C8 and C9 by fluorescence spectrophotometry

Fluorescence titration technique was used to examine the sensitivity. Since the optimum reaction time was 15 minutes, the fluorescence titration method was prepared batch by batch. Various concentrations of long-chain aldehydes including **C8** and **C9** (0-2 mM in DMSO) were added into the solution of **HNP5A** (1×10^{-5} M) adjusted with acetate buffer to receive 10% v/v DMSO/ acetate buffer (0.01 M, pH 4) of 3 mL final volume. After stirring for 15 minutes, the fluorescence spectra were recorded by fluorescence spectrophotometry.

According to the reported method, the calibration curves were created by graphing the fluorescence intensity at maximum wavelength versus different concentrations of guests with linearity equations. The limit of detection (LOD) and limit of quantitation (LOQ) were calculated on the basis of 3σ/m and 10σ/m equations, respectively.[3] The σ was standard deviation from the fluorescence intensity of free **HNP5A** and the m was slope of sensitivity curve.

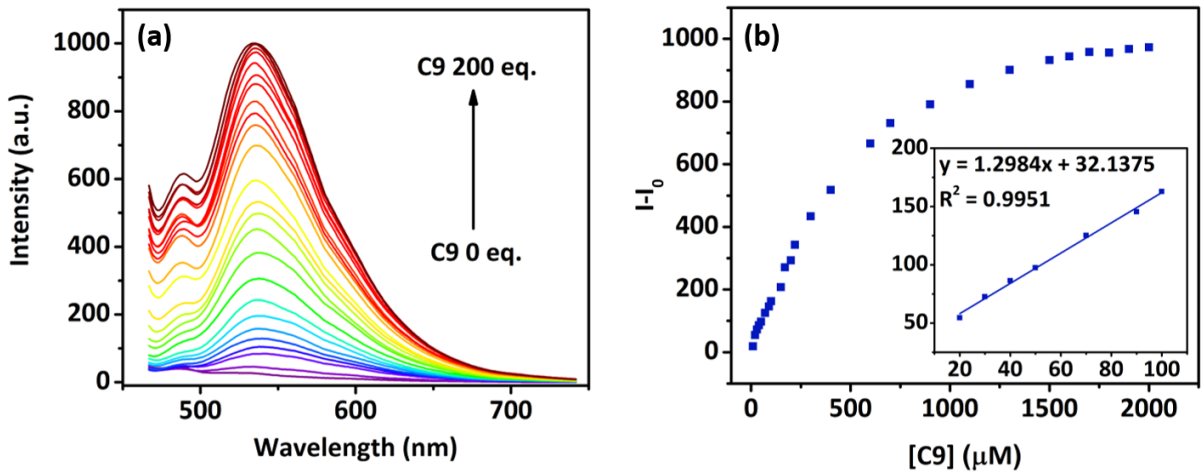

Figure S41 (a) Fluorescence titration spectra, (b) relative fluorescence intensities at 530 nm, and (inset) linear equation of **HNP5A** towards **C9** in 10% v/v DMSO/acetate buffer (0.01 M, pH4) (λ_{ex} = 438 nm, PMT 600 V, slit width 10 nm).

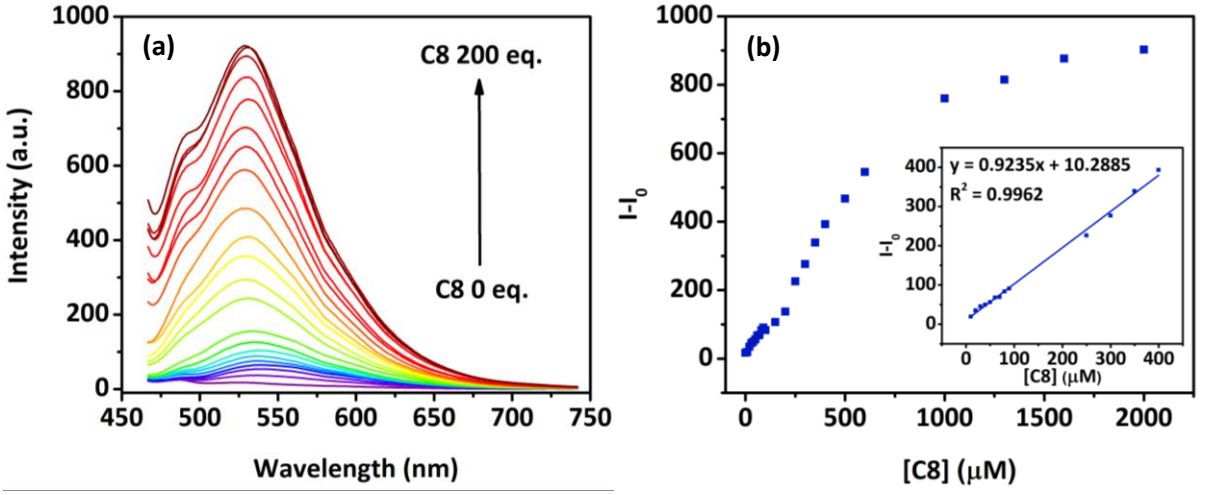

Figure S42 (a) Fluorescence titration spectra, (b) relative fluorescence intensities at 530 nm, and (inset) linear equation of **HNP5A** towards **C8** in 10% v/v DMSO/acetate buffer (0.01 M, pH4) (λ_{ex} = 438 nm, PMT 600 V, slit width 10 nm).

The fluorescence intensity was slightly enhanced and steady around 200 equivalents after introducing **C8** from 0 to 200 equivalents (Fig. S42). The linear relationship was observed in the concentration range of 10 µM to 400 µM, which was expressed by linear function: y = 0.9235x + 10.2885 (R^2 = 0.9962) (inset Fig. S42(b)). As the mentioned methods, the estimated LOD and LOQ of **HNP5A** for **C8** were 1.15 µM and 3.83 µM.

8. Interference study in the process of C9 detection

For the interference study, each portion prepared in a quartz cuvette comprised of 1 × 10^{-5} M **HNP5A**, 2 mM **C9** and various interfering molecules. The competing molecules included aldehyde molecules (formaldehyde (**C1**), propionaldehyde (**C3**), butyraldehyde (**C4**), valeraldehyde (**C5**), hexanal (**C6**), heptanal (**C7**), octanal (**C8**)) as well as the compounds existing in plasma and exhale breath such as glucose (Glu), sucrose (**Suc**), lysine (**Lys**), phenylalanine (**Phe**), glutathione (**Gluta**), urea, NaCl, and acetone. The total volume of the mixture solution was adjusted to 3 mL in 10% v/v DMSO/acetate buffer (0.01 M, pH4).

In order to prepare each portion, the mixture solution of 150 µL of 0.2 mM **HNP5A** in DMSO, 30 µL of DMSO, 2,700 µL of 0.01 M acetate buffer pH 4.0, and 60 µL of 0.1 M **C9** in DMSO was added with 60 µL of 0.1 M competing compounds in buffer. Subsequently, the mixture solution was stirred for 15 minutes at room temperature. After completing the reaction, the fluorescence signals were collected using fluorescence spectrophotometry and the naked-eye investigation was also recorded under a wavelength of 365 nm UV light.

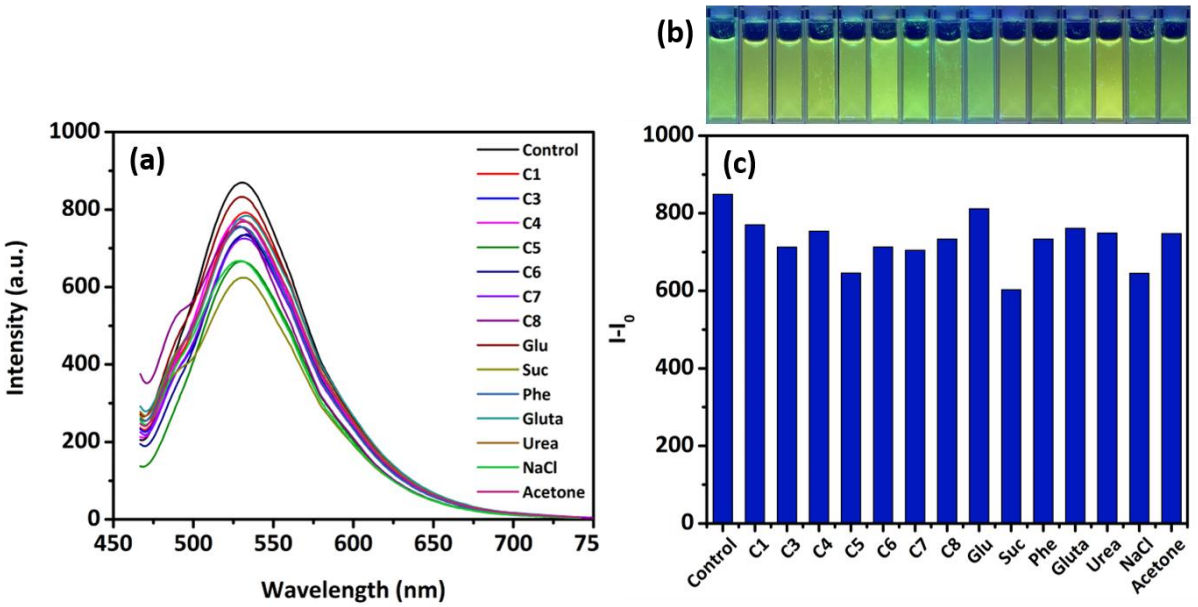

Figure S43 (a) Fluorescence spectra, (b) visual fluorescence, and (c) fluorescence intensities at 530 nm of **HNP5A⊂C9** as control and **HNP5A⊂C9** towards interfering compounds in 10% v/v DMSO/acetate buffer (0.01 M, pH 4) (λ_{ex} = 438 nm, PMT 590 V, slit width 10 nm).

9. Sensitivity study of HNP5A⊂C9 towards Ag ions (Ag^+) by fluorescence spectrophotometry

To prepare each portion, 150 µL of 0.2 mM **HNP5A** (1×10^{-5} M), 90 µL DMSO, and 2,600 µL of 0.01 M, pH 4 acetate buffer were mixed in a quartz cuvette. Then, a 60 µL of 0.1 M (2 mM) of **C9** in DMSO was added to the **HNP5A** solution and stirred for 15 minutes. The 100 µL of 0.06 M $AgNO_3$ in acetate buffer to get 3 mL of final volume was subsequently added and further stirred for 15 minutes. The fluorescence spectra were recorded and the naked eye detection was also recorded under a wavelength of 365 nm UV light.

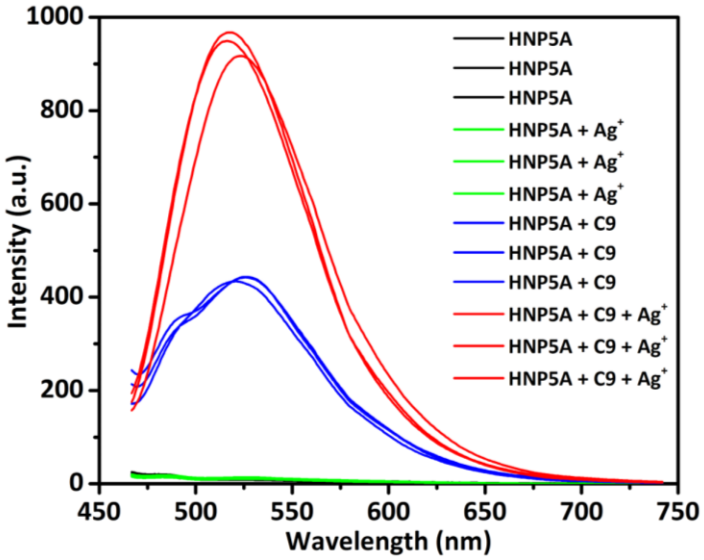

Figure S44 Fluorescence spectra of **HNP5A** in the presence of silver ions (**Ag^+**) and nonanal (**C9**) in 10% v/v DMSO/acetate buffer (0.01 M, pH 4). (λ_{ex} = 438 nm, PMT 570 V, slit width 10 nm).

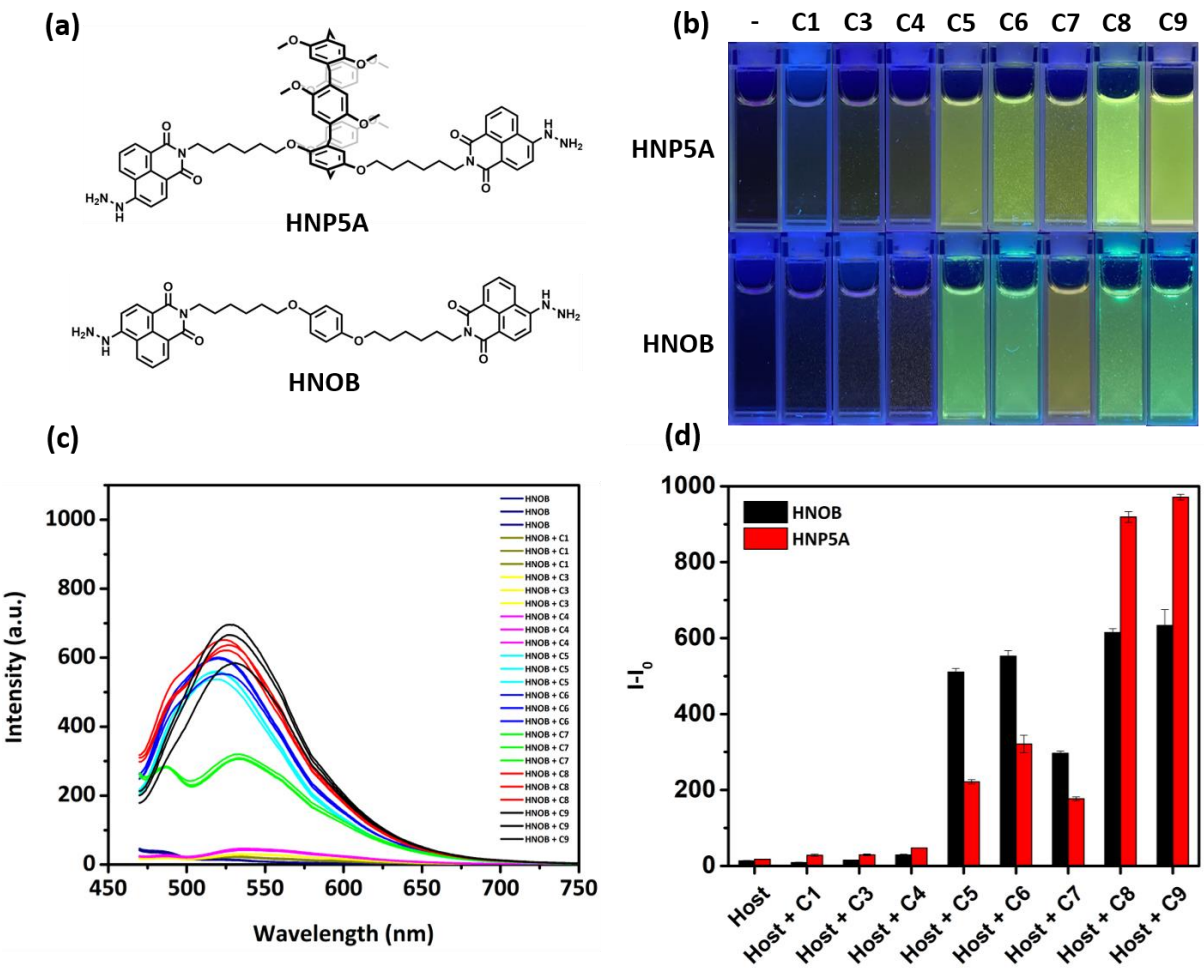

Figure S45 (a) Chemical structures, (b) visual fluorescence, (c) fluorescence spectra, and (d) fluorescence intensities of **HNP5A** and **HNOB** towards various aldehyde compounds at 530 nm, respectively in 10% v/v DMSO/acetate buffer (0.01 M, pH 4) (λ_{ex} = 438 nm (**HNP5A**), 441 nm (**HNOB**), PMT 590 V, slit width 10 nm).

To investigate selectivity of the fluorescence probe **HNOB** towards various aldehyde compounds, the detection was examined using fluorescence technique. From fluorescence intensity as showed in Fig. 3(a) and 3(c), the **HNOB** showed very weak fluorescence emission at 530 nm in 10% v/v DMSO/ acetate buffer (0.01 M, pH 4) as a result of two mechanisms combination: photoinduced electron transfer (PET) mechanism from lone pair electron of hydrazide group to napthalimide moiety and fluorescence resonance energy transfer (FRET) process from fluorophore to water molecules. When the long-chain aldehydes containing **C5**, **C6**, **C7**, **C8** and **C9** molecules were introduced into the **HNOB** solution, the fluorescence emission at 530 nm were similarly enhanced with light green fluorescence. It could be explained that PET mechanism inhibition from hydrazine to napthalimide groups was occurred after forming hydrazone. At the same time, long alky chain moiety that is hydrophobic part enveloped napthalimide dye for dispersion in water media. On the contrary, the fluorescence signal of **HNOB** hardly changed after the addition of short-chain aldehydes group comprising **C1**, **C3**, and **C4,** and the complex solution had no fluorescence emission corresponding with naked eye detection in Fig. 3(b). As a result, the probe **HNOB** without pillar[5]arene structure displayed nonspecific detection and low sensitivity. Consequently, the pillar[5]arene part contained

sensor **HNP5A** is a key structure to enhance both sensitivity and selectivity for long chain aldehyde sensing.

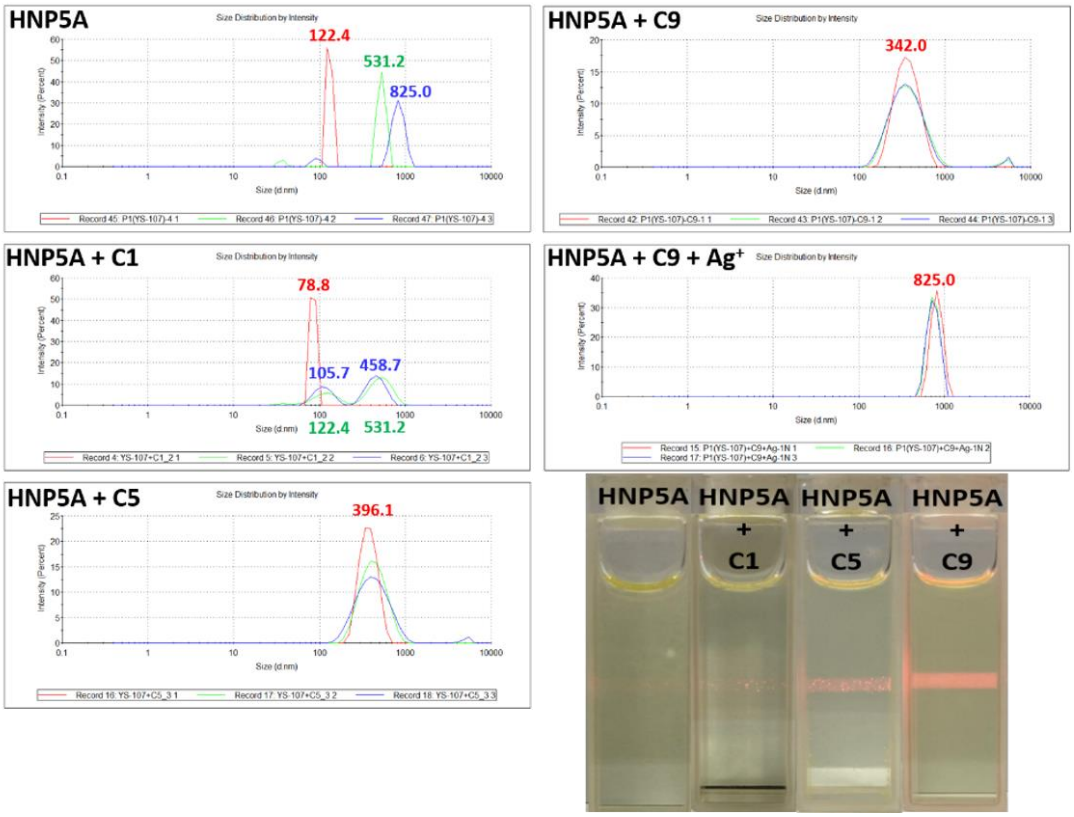

Figure S46 The DLS results of **HNP5A** with various guests in aqueous solution and the Tyndall effect in **HNP5A** and **HNP5A** in the presence of **C1**, **C5**, and **C9**.

10. Particle size verification of HNP5A, HNP5A⊂C9, and AgNPs-HNP5A⊂C9 by DLS measurement

For dynamic light scattering (DLS) measurement, firstly, the free host **HNP5A** (150 µL of 0.2 mM) was diluted with mixing of 150 µL DMSO and 2,700 µL to obtain a concentration of 1×10^{-5} M in 10% v/v DMSO/acetate buffer (0.01 M, pH 4). Then, a 60 µL of 0.1 M (2 mM) of **C9** in DMSO was introduced in the mixture of the 150 µL of 0.2 mM **HNP5A** (1×10^{-5} M), 90 µL DMSO, and 2,700 µL acetate buffer (0.01 M, pH 4) and stirred for 15 minutes. For the last portion, the 100 µL of 0.06 M $AgNO_3$ in acetate buffer was added to the mixture solution of 150 µL of 0.2 mM **HNP5A** (1×10^{-5} M), 90 µL DMSO, 2,600 µL acetate buffer (0.01 M, pH 4), and 60 µL of 0.1 M (2 mM) of **C9** in DMSO. The mixture solution was further stirred for 15 minutes. Each portion was measured by DLS technique at least three times under 25 °C.

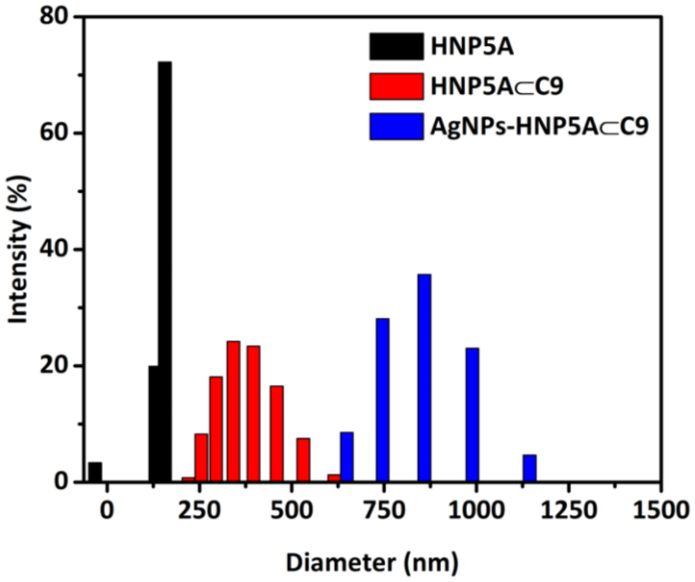

Figure S47 Size distribution graph of **HNP5A**, **HNP5A⊂C9**, **AgNPs-HNP5A⊂C9**.

Table S1 Particle size and PDI values of **HNP5A**, **HNP5A⊂C9**, **AgNPs-HNP5A⊂C9**.

Compound	Z-Ave (d.nm)	PDI
HNP5A	178.53 ± 31.75	1.00 ± 0.05
HNP5A⊂C9	372.57 ± 2.11	0.16 ± 0.03
AgNPs-HNP5A⊂C9	788.23 ± 43.82	0.25 ± 0.13

11. Morphology characterization and size distribution of HNP5A, HNP5A⊂C9, HNP5A + Ag^+, and AgNPs-HNP5A⊂C9 by FESEM and HRTEM techniques

Sample preparation for SEM and TEM, the free host **HNP5A** (150 µL of 0.2 mM) was diluted with a mixing of 150 µL DMSO and 2,700 µL to receive a concentration of 1×10^{-5} M in 10% v/v DMSO/acetate buffer (0.01 M, pH 4). Then, a 60 µL of 0.1 M (2 mM) of **C9** in DMSO was introduced in the mixture of the 150 µL of 0.2 mM **HNP5A** (1×10^{-5} M), 90 µL DMSO, and 2,700 µL acetate buffer (0.01 M, pH 4) and stirred for 15 minutes. For **HNP5A + Ag^+**, the 100 µL of 0.06 M $AgNO_3$ in acetate buffer was added to the solution of 150 µL of 0.2 mM **HNP5A** (1×10^{-5} M), 150 µL DMSO, 2,600 µL acetate buffer (0.01 M, pH 4), and stirred for 15 minutes. In the last portion, the 100 µL of 0.06 M $AgNO_3$ in acetate buffer was added to the mixture solution of 150 µL of 0.2 mM **HNP5A** (1×10^{-5} M), 90 µL DMSO, 2,600 µL acetate buffer (0.01 M, pH 4), and 60 µL of 0.1 M (2 mM) of **C9** in DMSO after 15 minutes of stirring time. The mixture solution was further stirred for 15 minutes. Each sample was centrifuged at 10,000 rpm for 15 minutes, washed with milli Q water (1000 µL × 3) to remove residue substances, and dispersed in 500 µL milli Q water.

To prepare sample for SEM analysis, 5 µL of each sample was drop-casted on the smooth aluminum foil and left until dry in silica gel overnight. All samples were coated with Pt/Pd for conducting before analysis. In the case of TEM, 5 µL of each sample was drop-casted on carbon side of copper grid and allowed to dry in silica gel overnight. TEM analysis was further recorded.

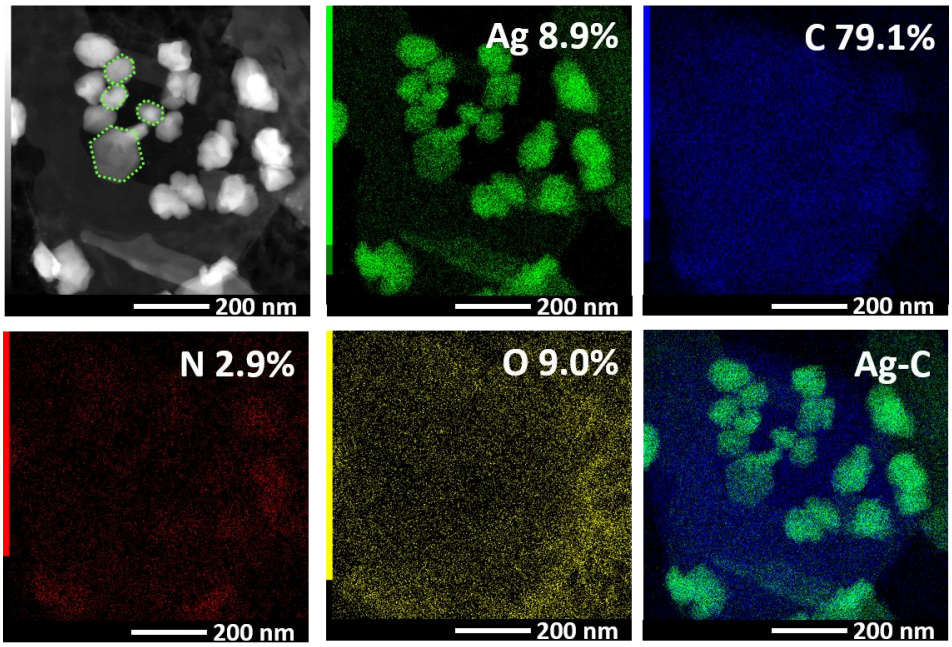

Figure S48 EDX mapping of **AgNPs-HNP5A⊂C9**.

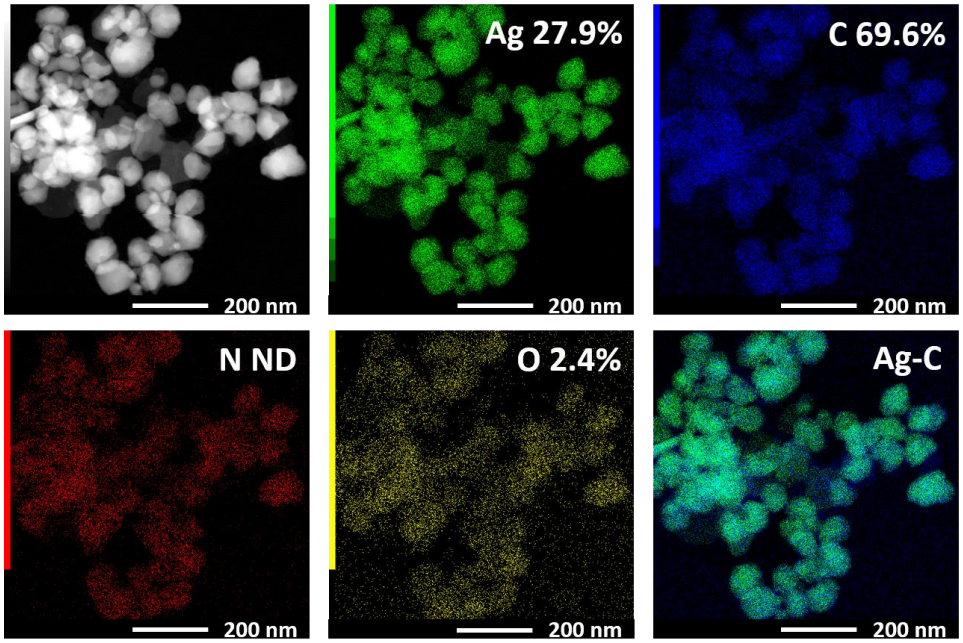

Figure S49 EDX mapping of **HNP5A** + Ag^{+}.

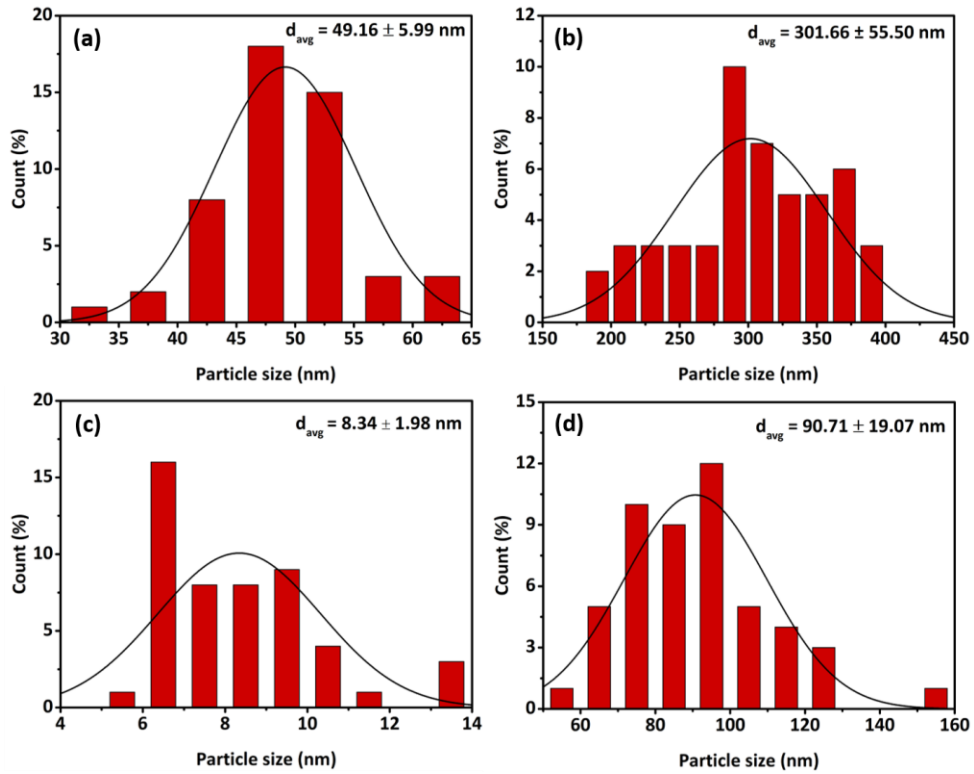

Figure S50 Histograms of the size distribution for (a) **HNP5A**, (b) **HNP5A⊂C9,** (c) and (d) **AgNPs-HNP5A⊂C9**.

12. DFT Optimized structures and reaction energies

Structures of various the monomers, dimer and trimer of bis-hydrazide napthalimide functionalized pillar[5]arene derivative (**HNP5A**) of **C9** methylene groups (**HNP5A⊂C9**) and related species were optimized using density functional theory (DFT) method [4]. The Becke's three parameter

hybrid functional [5] and the Lee–Yang–Parr correlation functional (B3LYP), [6] with 6–31G(d) basis set [7], called B3LYP/6–31G(d) method, were performed on structural optimization calculations. Total energies of B3LYP/6–31G(d)-optimized structures were obtained using single-point of the PCM solvent effect (water) calculations [8]. The All calculations were performed with the Gaussian 09 program [9] and initial structures for all studied species were prepared and visualized using GaussView 5.0.9 program [10].

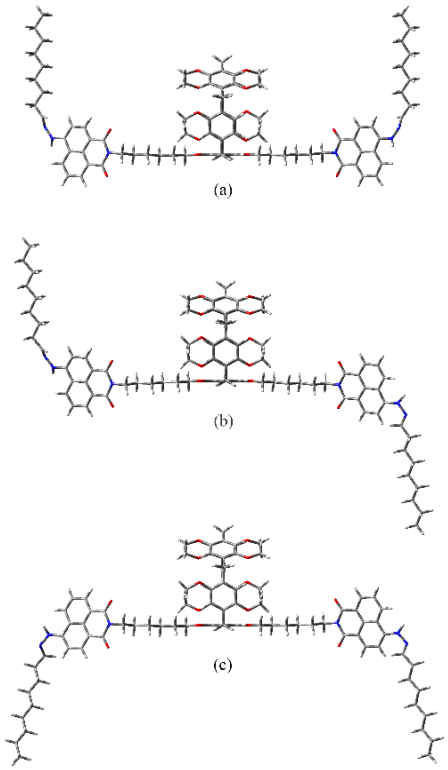

Figure S51 The B3LYP/6–31G(p)–optimized structures of monomeric conformers (a) **HNP5A⊂C9-W**, (b) **HNP5A⊂C9-S** and (c) **HNP5A⊂C9-M**.

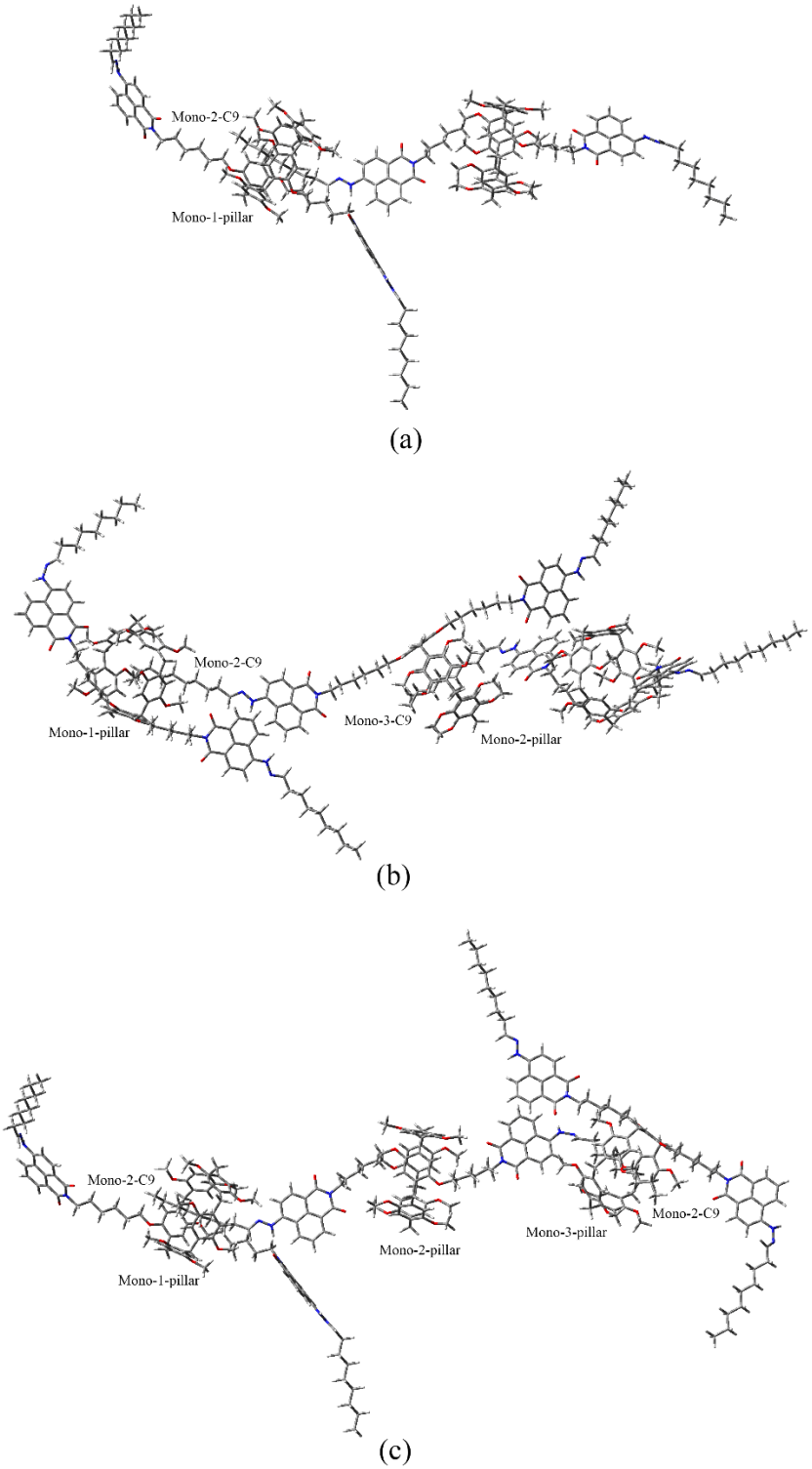

Figure S52 The B3LYP/6–31G(p)–optimized structures of (a) the most stable dimer (**HNP5A⊂C9**)$_2$, (b) the most stable trimeric structures of type I [(**HNP5A⊂C9**)$_3$-I] and (c) type II [(**HNP5A⊂C9**)$_3$-II].

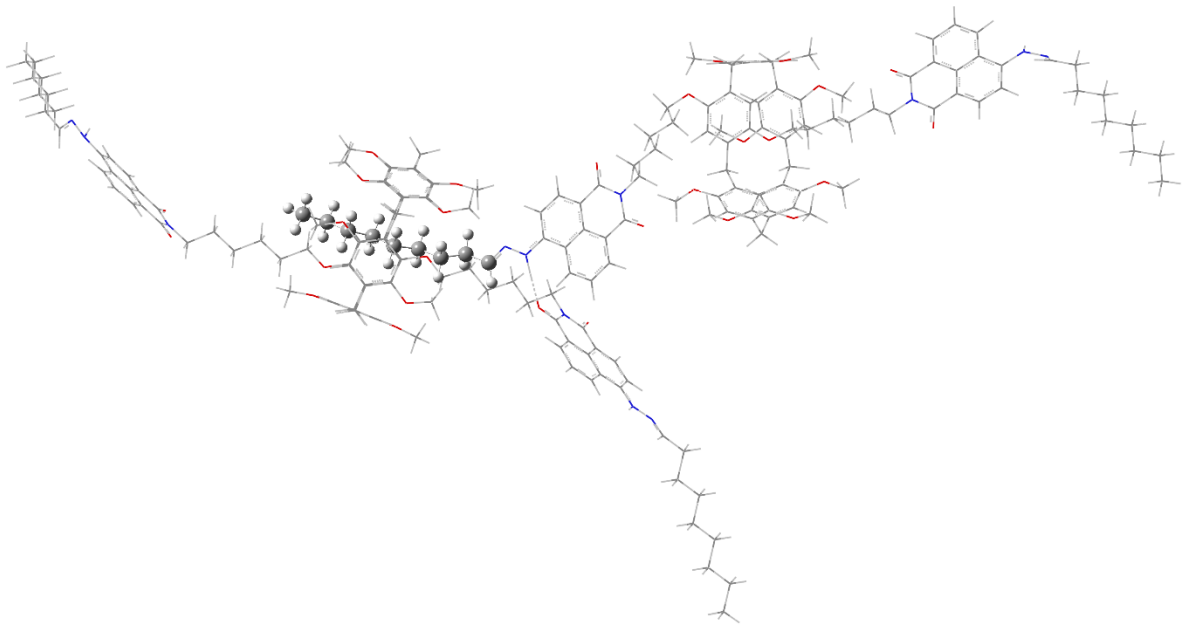

Figure S53 Aggregation of two **HNP5A⊂C9** monomers to form dimer, the pillar[5]arene channel of the first **HNP5A⊂C9** monomer (the left) is inserted by a C9-terminal of the second **HNP5A⊂C9** monomer (the right).

Table S2 Total energies of conformers of monomer, dimer, and trimer of **HNP5A⊂C9** in water, their relative energies, frontier orbital energies and energy gaps, computed by the PCM/B3LYP/6–31G(d) method.

Species	E_{total}, au	ΔE_{rel}, kcal/mol	Reaction, kcal/mol	E_{gap}, eV	$\Delta E_{gap,\%}$ [a]
Monomer:					
HNP5A⊂C9-W	-5147.8940299	0.085 [b]	-	-2.890	-
HNP5A⊂C9-S	-5147.8941545	0.000 [b]	-	-2.887	-
HNP5A⊂C9-M	-5147.8938996	0.069 [b]	-	-2.884	-
Dimer:					
(**HNP5A⊂C9**)$_2$	-10295.8050008	-[c]	-10.47	-2.834	-1.85
Trimer:					
[(**HNP5A⊂C9**)$_3$-I]	-15443.7217378	-[c]	-14.17	-2.839	-1.67

[a] The change of energy gap of the most stable conformer **HNP5A⊂C9-S**

[b] The total energies compared with the most stable conformer **HNP5A⊂C9-S**

[c] The most stable conformers

[d] The total energies compared with the most stable conformer of type I [(**HNP5A⊂C9**)$_3$-I]

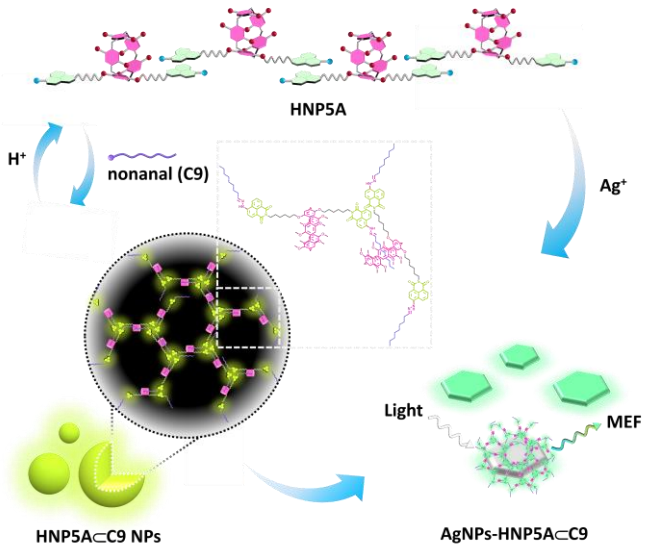

Scheme S1 Proposed sensing mechanism of the sensor **HNP5A** in the presence of nonanal (**C9**) and Ag^{+}.

13. References

1. Q. Lin, Y. Q. Fan, P. P. Mao, L. Liu, J. Liu, Y. M. Zhang, H. Yao and T. B. Wei, *Chemistry*, 2018, **24**, 777-783.
2. L. Liu, D. Cao, Y. Jin, H. Tao, Y. Kou and H. Meier, *Org. Biomol. Chem.*, 2011, **9**, 7007-7010.
3. A. Shrivastava and V. Gupta, *Chron. Young Sci.*, 2011, **2**.
4. W. Kohn and L. J. Sham, *Phys. Rev.*, 1965, **140**, A1133-A1138.
5. A. D. Becke, *J. Chem. Phys.*, 1993, **98**, 5648-5652.
6. C. Lee, W. Yang and R. G. Parr, *Phys. Rev. B*, 1988, **37**, 785-789.
7. R. Ditchfield, W. J. Hehre and J. A. Pople, *J. Chem. Phys.*, 1971, **54**, 720-723.
8. G. Scalmani and M. J. Frisch, *J. Chem. Phys.*, 2010, **132**.
9 M.J. Frisch, et al., Gaussian 09, Revision D.01, Gaussian, Inc., Wallingford, CT, 2014.
10. R. Dennington, T. Keith and J. Millam, GaussView 5, Semichem Inc, Shawnee Mission,. KS 2009.